# Fluorescent Iridium(III) Coumarin-salicylaldehyde Schiff Base Compounds as Lysosome-Targeted antitumor agents

Cong Liu, Xicheng Liu*, Xingxing Ge, Qinghui Wang, Lei Zhang, Wenjing Shang, Yue Zhang, XiangAi Yuan, Laijin Tian, Zhe Liu*, Jinmao You

*Institute of Anticancer Agents Development and Theranostic Application, The Key Laboratory of Life-Organic Analysis and Key Laboratory of Pharmaceutical Intermediates and Analysis of Natural Medicine, School of Chemistry and Chemical Engineering, Qufu Normal University, Qufu 273165, China.*

*Corresponding authors (*Email*): chemlxc@163.com (X. C. Liu); liuzheqd@163.com (Z. Liu)

## Supporting Information

## EXPERIMENTAL SECTION

### NMR Spectrum

NMR spectra were acquired in 5 mm NMR tubes at 298 K on Bruker DPX 500 ($^{1}$H NMR: 500.13 MHz; $^{13}$C NMR: 126 MHz; $^{19}$F NMR: 471 MHz) spectrometers. $^{1}$H NMR chemical shifts were internally referenced to $CHCl_3$ (7.26 ppm) for chloroform-$d_1$, and 77.41 ppm, 77.16 ppm, 76.91 ppm for $^{13}$C NMR. All data was carried out using XWIN-NMR version 3.6 (Bruker UK Ltd.).

### X-ray Crystallography

All diffraction data were obtained on a Bruker Smart Apex CCD diffractometer equipped with graphite-monochro mated Mo Kα radiation. Absorption corrections were applied using SADABS program. SQUEEZE option was used to remove the non-localized electron density at the final step of structure refinement. The structures were solved by direct methods using SHELXS (TREF) with additional light atoms found by Fourier methods. Complexes were refined against *F*2 using SHELXL, and hydrogen atoms were added at calculated positions and refined riding on their parent atoms. X-ray crystallographic data for **Ir1** and **Ir4** are available as Figure 2, Table S1 has been deposited in the Cambridge Crystallographic Data Centre under the accession numbers CCDC 1970999 and 1971001, respectively. X-ray crystallographic data in CIF format are available from the Cambridge Crystallographic Data Centre.

### Computational Details

All the calculations were performed with the Gaussian 09 program packages[1] in solution-phase with PCM solvent model[2,3] (solvent = DMSO). The starting structures were obtained from the crystal structures. B3LYP[4,5] and M06-2X functional were used for the DFT calculations. The triple-ζ quality basis set 6–311G** was employed for all nonmetal atoms. The LANL2TZ basis set including a triple-$\zeta$ valence basis set with the Hay and Wadt effective core potential (ECP) was used for Iridium with an f polarization function of exponent 0.938. Frequency calculations at the same level of theory were carried out to characterize each stationary point (minimum). The WBI (Wiberg bond index) values were calculated in Natural Bond Orbital (NBO) analysis using the keywords pop =NBORead, which were useful tools to estimate the bond order between two atoms. The time-dependent density functional theory (TDDFT)[6,7] was employed to calculate the absorption spectra of these Ir complexes with M06-2X[8] functional and the same basis sets as

above in PCM solvent model[2,3].

**UV-vis Spectroscopy**

UV-vis spectra of these compounds were recorded by TU-1901 UV spectrophotometer with 1 cm path-length quartz cuvettes (3 mL). Spectra were processed using UV Winlab software. Experiments were carried out at 298 K unless otherwise stated.

**Reaction with NADH**

The reaction of compounds **Ir1-Ir6** (ca. 1 $\mu$M) with NADH (ca. 100 $\mu$M) in 10% MeOH/90% $H_2O$ (*v*/*v*) was monitored by UV-vis at 298 K after various time intervals. TONs were calculated from the difference in NADH concentration after 8 h divided by the concentration of iridium catalyst. The concentration of NADH was obtained using the extinction coefficient $\varepsilon_{339} = 6220\ M^{-1}cm^{-1}$.

**Cell Culture**

A549 (lung cancer cells), Hela (cervical cancer cell) and BEAS-2B (human normal lung epithelial cells) were obtained from Shanghai Institute of Biochemistry and Cell Biology (SIBCB) and were grown in Dubelco's Modified Eagle Medium (DMEM). All media were supplemented with 10% fetal bovine serum, and 1% penicillin-streptomycin solution. All cells were grown at 310 K in a humidified incubator under 5% $CO_2$ atmosphere.

**MTT assay**

After plating 5000 cells per well in 96-well plates, the cells were preincubated in drug-free media at 310 K for 24 h before adding different concentrations of the compounds to be tested. In order to prepare the stock solution of the drug, the solid compound was dissolved in DMSO. This stock was further diluted using cell culture medium until working concentrations were achieved. The drug exposure period was 24 h. Subsequently, 15 $\mu$L of 5 mg $mL^{-1}$ MTT solution was added to form a purple formazan. Afterwards, 100 $\mu$L of dimethyl sulfoxide (DMSO) was transferred into each well to dissolve the purple formazan, and results were measured using a microplate reader (DNM-9606, Perlong Medical, Beijing, China) at an absorbance of 570 nm. Each well was triplicated and each experiment repeated at least three times. $IC_{50}$ values quoted are mean ± SEM.

**Antimetastatic Properties.**

A549 cells (1, 500, 000 per well) were seeded in 2000 $\mu$L media in 6-well plates and allowed to attach and grow to form a confluent monolayer. Each well of the plates was marked with a horizontal line passing through the center of bottom in advance. Wounds were created perpendicular to the lines by 10 $\mu$L tips, and unattached cells were removed by washing with PBS (pH = 7.4). **Ir2** and **Ir5** in DMEM with 1% FBS was added and cells incubated at 37 ºC under 5% $CO_2$ for imaging. DMEM with 1% FBS was used to suppress cell proliferation. Images were captured at 0 and 24 h at the same position of each well. Experiments were repeated for at least three times.

**ROS Determination**

Flow cytometry analysis of ROS generation in A549 cells caused by exposure to iridium compounds were carried out using the Reactive Oxygen Species Assay Kit (Beyotime Institute of Biotechnology, Shanghai, China) according to the supplier's instructions. Briefly, $1.5 \times 10^6$ A549 cells per well were seeded in a six-well plate. Cells were preincubated in drug-free media at 310 K for 24 h in a 5% $CO_2$ humidified atmosphere, and then drugs were added at concentrations of $0.25 \times IC_{50}$ and $0.5\times IC_{50}$. After 24 h of drug exposure, cells were washed twice with PBS and then incubated with the DCFH-DA probe (10 $\mu$M) at 37 °C for 30 min, and then washed triple immediately with PBS. The fluorescence intensity was analyzed by flow cytometry (ACEA NovoCyte, Hangzhou, China). Data were processed using NovoExpress™ software. Samples were kept under dark conditions to avoid light-induced ROS production.

**Cell Cycle Analysis**

The A549 cancer cells at $1.5 \times 10^6$ per well were seeded in a six-well plate. Cells were preincubated in drug-free media at 310 K for 24 h, then **Ir2** and **Ir5** were added at concentrations of $0.25 \times IC_{50,}$ $0.5 \times IC_{50}$ and $1.0 \times IC_{50}$ of **Ir2** and **Ir5** against A549 cells. After 24 h of exposure, supernatants were removed by suction and cells were washed with PBS. Finally, cells were harvested using trypsin-EDTA and fixed for 24 h using cold 70% ethanol. DNA staining was achieved by suspending the cell pellets in PBS containing propidium iodide (PI) and RNAse. Cell pellets were washed and suspended in PBS before being analyzed in a flow cytometer (ACEA NovoCyte, Hangzhou, China) using excitation of DNA-bound PI at 488 nm, with emission at 585 nm. Data were processed using NovoExpress™ software. The cell cycle distribution is shown as the percentage of cells containing $G_0/G_1$, S and $G_2$/M DNA as identified by propidium iodide staining.

**Induction of Apoptosis**

Flow cytometry analysis of apoptotic populations of the cells caused by exposure to iridium compounds were carried out using the Annexin V-FITC Apoptosis Detection Kit (Beyotime Institute of Biotechnology, China) according to the supplier's instructions. Briefly, A549 cells ($1.5 \times 10^6$/2 mL per well) were seeded in a six-well plate. Cells were preincubated in drug-free media at 310 K for 24 h, after which **Ir2** and **Ir5** was added at concentrations of $1.0 \times IC_{50}$, $2.0 \times IC_{50}$ and $3.0 \times IC_{50}$ of **Ir2** and **Ir5** against A549 cells. After 24 h of drug exposure, cells were collected, washed once with PBS, and suspended in 195 $\mu$L of annexin V-FITC binding buffer which was then added to 5 $\mu$L of annexin V-FITC and 10 $\mu$L of PI, and then incubated at room temperature in the dark for 15 min. Subsequently, the buffer placed in an ice bath in the dark. The samples were analyzed by a flow cytometer (ACEA NovoCyte, Hangzhou, China).

**Mitochondrial Membrane Potential Assay**

Analysis of the changes of mitochondrial potential in cells after exposure to iridium compounds was carried out using the mitochondrial membrane potential assay kit with JC-1 (Beyotime Institute of Biotechnology, Shanghai, China) according to the manufacturer's instructions. Briefly, $1.5 \times 10^6$ A549 cells were seeded in six-well plates left to incubate for 24 h in drug-free medium at 310 K in a humidified atmosphere. Drug solutions, with the concentration changed from $0.25 \times IC_{50}$ to $2.0 \times IC_{50}$ of **Ir2** and **Ir5** against A549 cancer cells, were added in triplicate, and the cells were left to incubate for a further 24 h under similar conditions. Supernatants were removed by suction, and each well was washed with PBS before detaching the cells using trypsin-EDTA. Staining of the samples was done in flow cytometry tubes protected from light, incubating for 30 min at ambient temperature. The samples were immediately analyzed by a flow cytometer (ACEA NovoCyte, Hangzhou, China). For positive controls, the cells were exposed to carbonyl cyanide 3-chlorophenylhydrazone, CCCP (5 $\mu$M), for 20 min. Data were processed using NovoExpress™ software.

**Cellular Localization Assay**

Two Photon Laser Scanning Microscope (*/LSM/880NLO) is produced at Carl Zeiss AG, Germany. LTDR (Life Technologies, USA), MTDR (Life Technologies, USA), CCCP (Sigma Aldrich, USA), chloroquine (Sigma Aldrich, USA) were used as received. A549 cells were seeded into 35 mm dishes (Greiner, Germany) for confocal microscopy. After cultured overnight, the cells were incubated with compounds **Ir2** and **Ir5** ($1.0 \times IC_{50}$) for 1 h. The treated cells were

observed immediately under a confocal microscope with excitation at 405 nm. For colocalization studies, the cells were incubated with compounds (1.0 × $IC_{50}$) for 1 h. Subsequently, the medium was replaced with staining medium containing MTDR/LDTR and stained for another 20 min and 1 h.The cells were washed twice with PBS, and then viewed immediately under a confocal microscope.

**Assay for the lysosomal membrane permeabilization (Acridine Orange assay)**

A549 cells seeded into six-well plate (Corning) were exposed to **Ir2** and **Ir5** at the indicated concentrations for 12 h. The cells were then washed twice with PBS and incubated with AO (5 $\mu$M) at 37 °C for 15 min. The cells were washed twice with PBS and visualized by confocal microscopy (LSM/880NLO). Emission was collected at 510 ± 20 nm (green) and 625 ± 20 nm (red) upon excitation at 488 nm.

**Cellular Uptake Studies**

A549 cells were seeded in 35 mm dishes for 24 h and at 4 °C or preincubated with CCCP (10 $\mu$M) or chloroquine (50 $\mu$M) for 1 h. The medium was removed and the cells were then incubated with **Ir2** and **Ir5** (1.0 × $IC_{50}$) for 15 min. The cells were washed three times with ice-cold PBS and visualize by confocal microscopy (LSM/880NLO) immediately.

## SYNTHESIS

*Synthesis of* $[(\eta^5\text{-}C_5Me_5)IrCl_2]_2$ ***(Dimer1)***, $[(\eta^5\text{-}C_5Me_4C_6H_5)IrCl_2]_2$ ***(Dimer2)*** *and* $[(\eta^5\text{-}C_5Me_4C_6H_4C_6H_5)IrCl_2]_2$ ***(Dimer3)***

$IrCl_3{\cdot}3H_2O$ (0.50 g, 1.7 mmol) was dissolved in MeOH (20 mL) in a microwave vial, pentamethyl cyclopentadiene (0.69 g, 5.0 mmol) was added and reacted at 127 °C, 400 psi for 30 min in a microwave instrument. The reaction mixture was allowed to cool to ambient temperature and the dark green precipitate was filtered off. The volume of the dark red filtrate was reduced to ca. 15 mL on a rotary evaporator. Upon cooling to ambient temperature, an orange precipitate appeared and was collected by filtration. The product was washed with methanol and diethyl ether, dried in air, and pure **Dimer 1** was obtained. Yield: 0.88 g (65%). $^1$H NMR (500 MHz, $CDCl_3$): δ 1.60 (s, $J$ = 1.4 Hz, 15H).

**Dimer 2** and **Dimer 3** were synthesized using phenyltetramethyl cyclopentadiene (0.99 g, 5.0 mmol)/biphenyltetramethyl cyclopentadiene (1.37 g, 5.0 mmol) and $IrCl_3{\cdot}3H_2O$ (0.50 g, 1.7

mmol) according to the method of **Dimer 1**. The data were listed as follows:

**Dimer2**: Yield: 0.91 g (58.5%). $^1$H NMR (500 MHz, $CDCl_3$): δ 7.58 (m, 2H), 7.35 (m, 3H), 1.72 (s, 6H), 1.63 (s, 6H)

**Dimer3**: Yield: 1.15 g (63.4%). 1 H NMR (500 MHz, $CDCl_3$): δ 7.64 (m, 4H), 7.44 (m, 2H), 7.33 (m, 3H), 3.25 (m, 1H), 2.08 (s, 3H), 1.95 (s, 3H), 1.88 (s, 3H), 1.00 (d, *J* = 7.5 Hz, 3H).

*Synthesis of the [($\eta^5$-Cp$^x$)Ir(O^N)Cl]* ***(Ir7)***

To a 200 mL round bottom flask, 0.50 g (4.09 mmol) of salicylaldehyde and 0.38 g (4.09 mmol) of aniline were added, respectively. To the above flask, 40 ml of anhydrous methanol was added and added dropwise, 1 d formic acid as a catalyst. The mixed system was stirred and refluxed at 70 ℃ for about 36 h until the reaction was complete. Then the above products (0.024 g, 0.12 mmol) reacted with **Dimer 1** (0.050 g, 0.06 mmol) and sodium acetate (0.033 g, 0.40 mmol) in nitrogen, and finally the control compound was obtained, Scheme S1. The $^1$H NMR and ESI-MS are shown in Figures S15-S16. Yield: 0.028 g (83%). $^1$H NMR (500 MHz, CDCl3): δ 8.02 (s, 1H), 7.68 (d, *J* = 7.9 Hz, 2H), 7.36 (dt, *J* = 20.3, 7.7 Hz, 4H), 7.11 (d, *J* = 7.8 Hz, 1H), 6.97 (d, *J* = 8.6 Hz, 1H), 6.45 (t, *J* = 7.3 Hz, 1H), 1.32 (s, 15H). ESI-MS (*m/z*): Calcd for $C_{23}H_{25}ONIr$: 523.6; Found: 524.2 $[M\text{-}Cl]^+$.

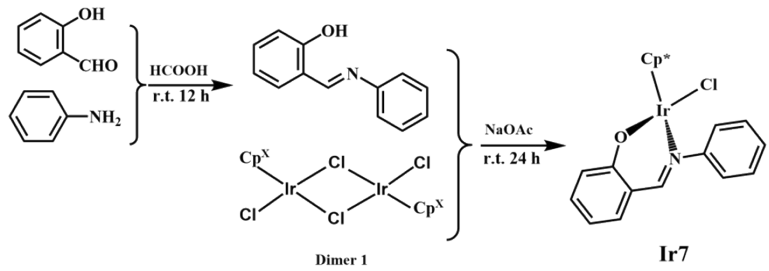


**Scheme S1.** Synthesis process of **Ir7**.

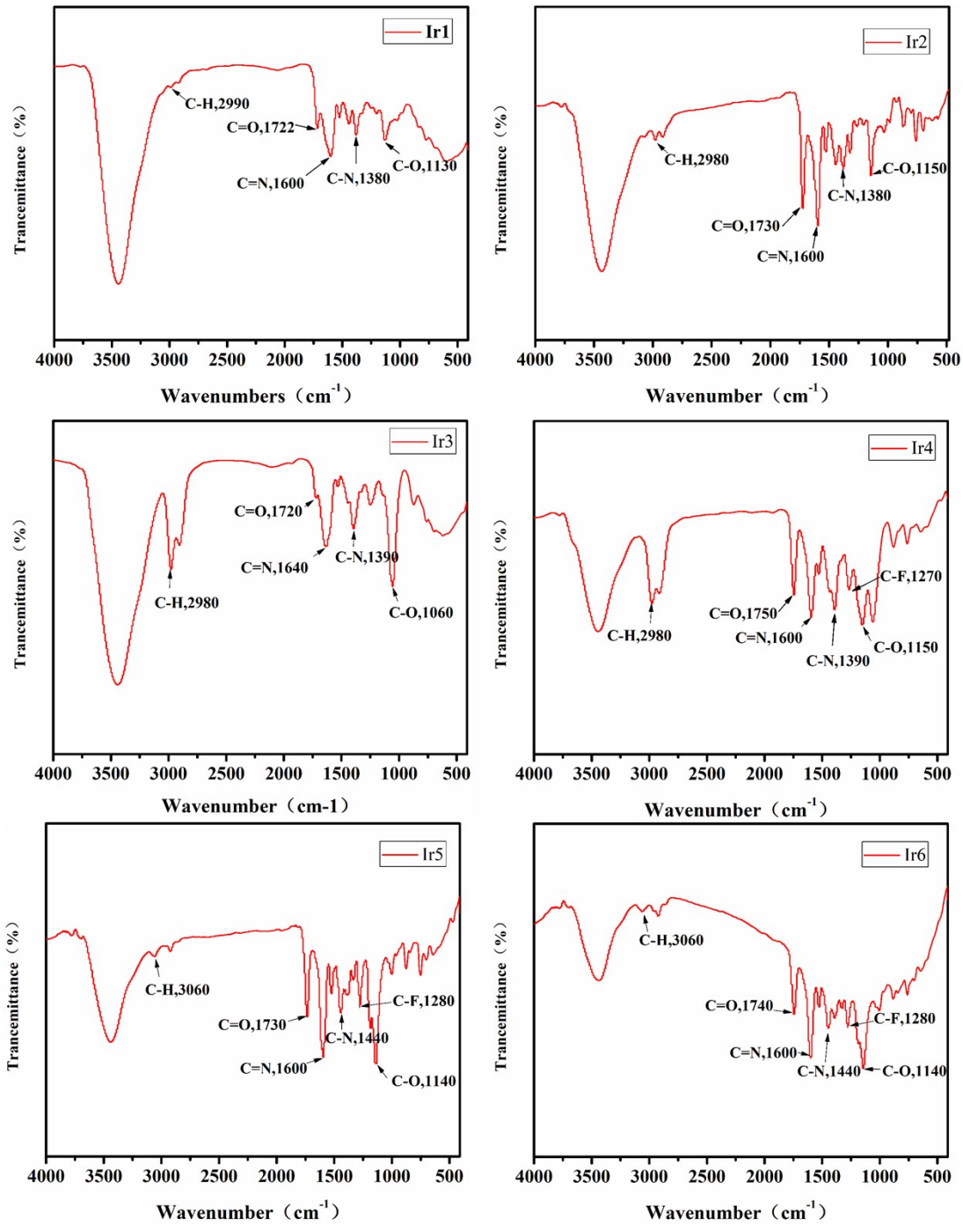


**Figure S1.** FT-IR spectra of **Ir1-Ir6**.

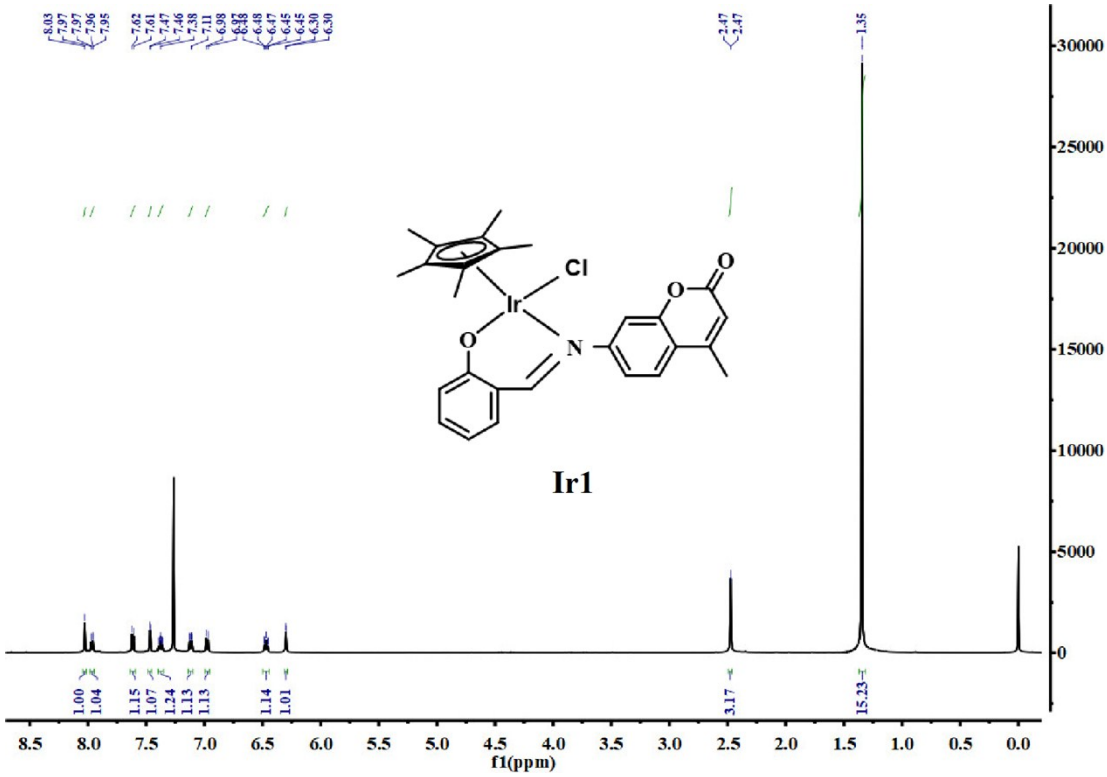
Cl
Ir
O
N
O
O
Ir1
f1(ppm)

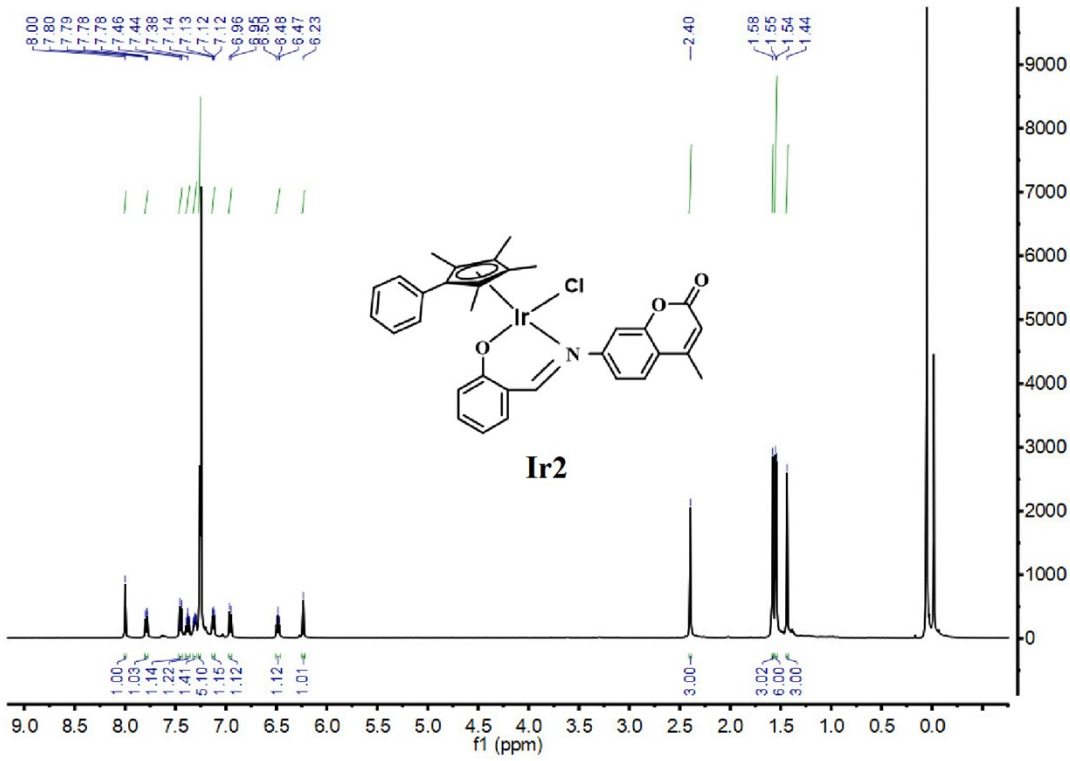
Cl
Ir
O
N
O
O
Ir2
f1 (ppm)

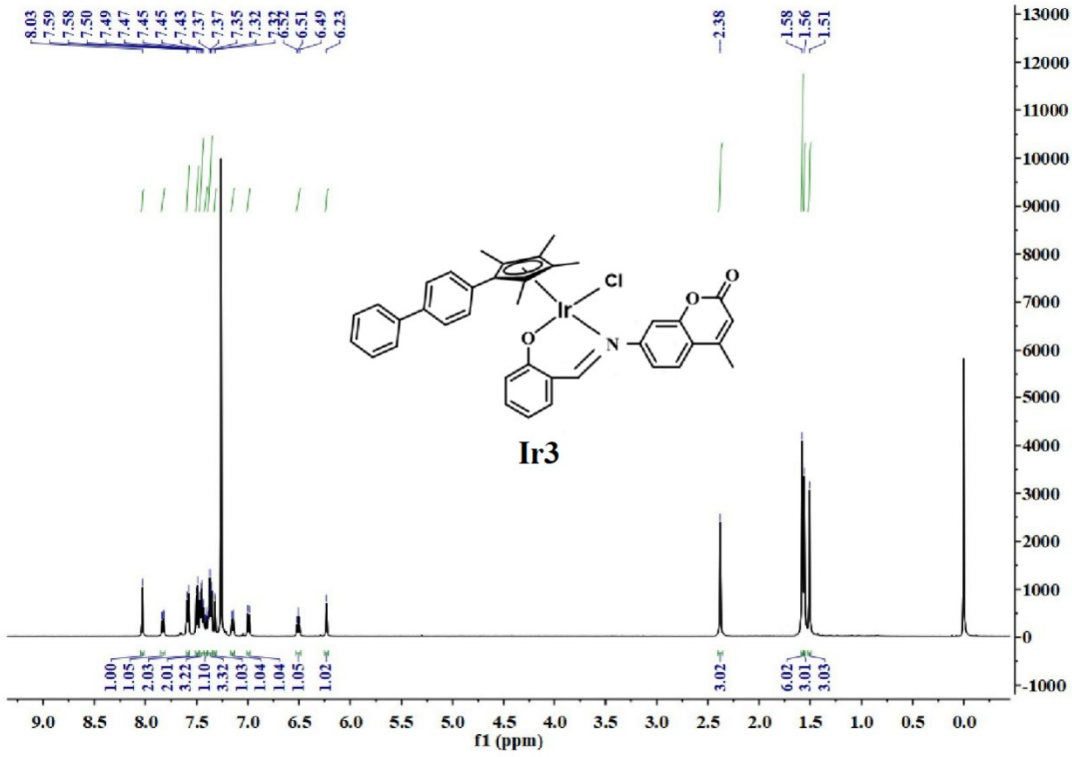
Cl
Ir
O
N
O
O
Ir3
f1 (ppm)

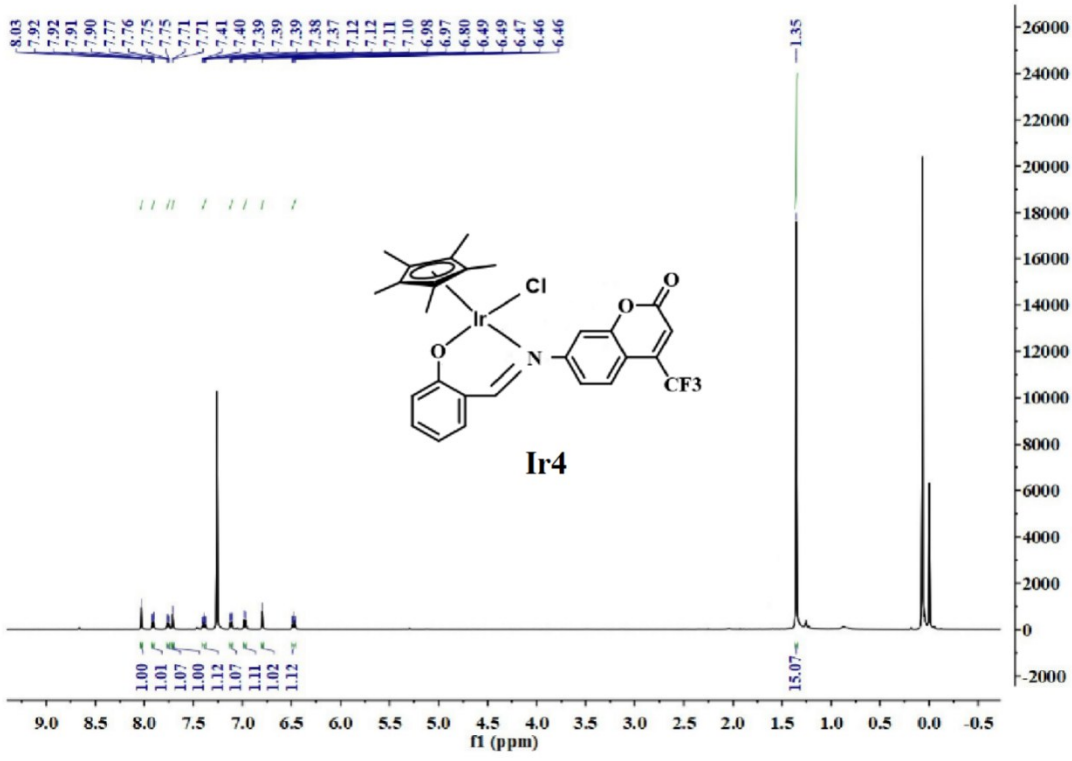
Cl
Ir
O
N
O
O
CF3
Ir4
f1 (ppm)

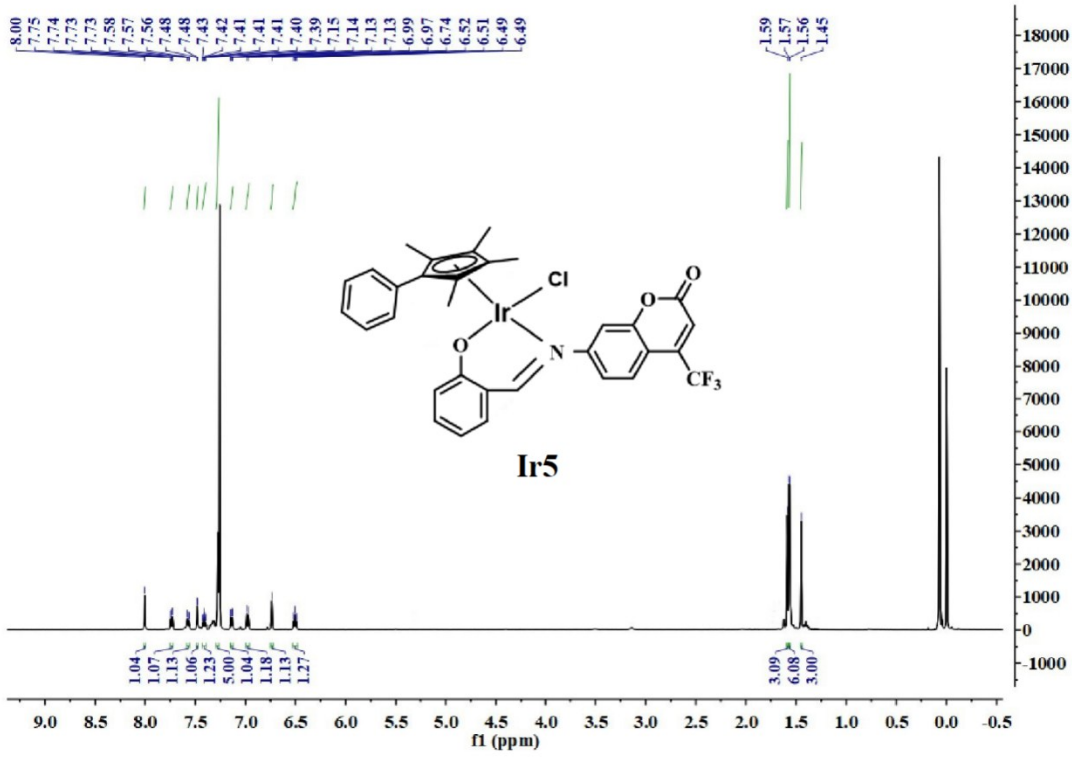


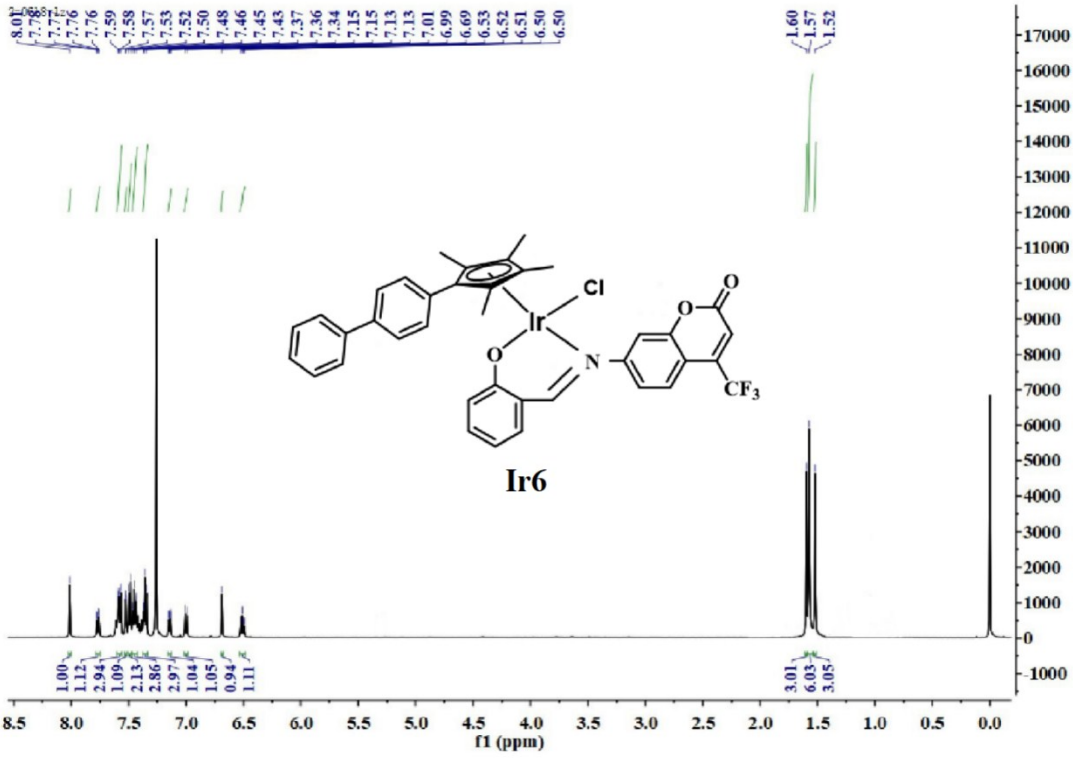


**Figure S2.** $^{1}$H NMR spectra (500 MHz) of **Ir1-Ir6**.

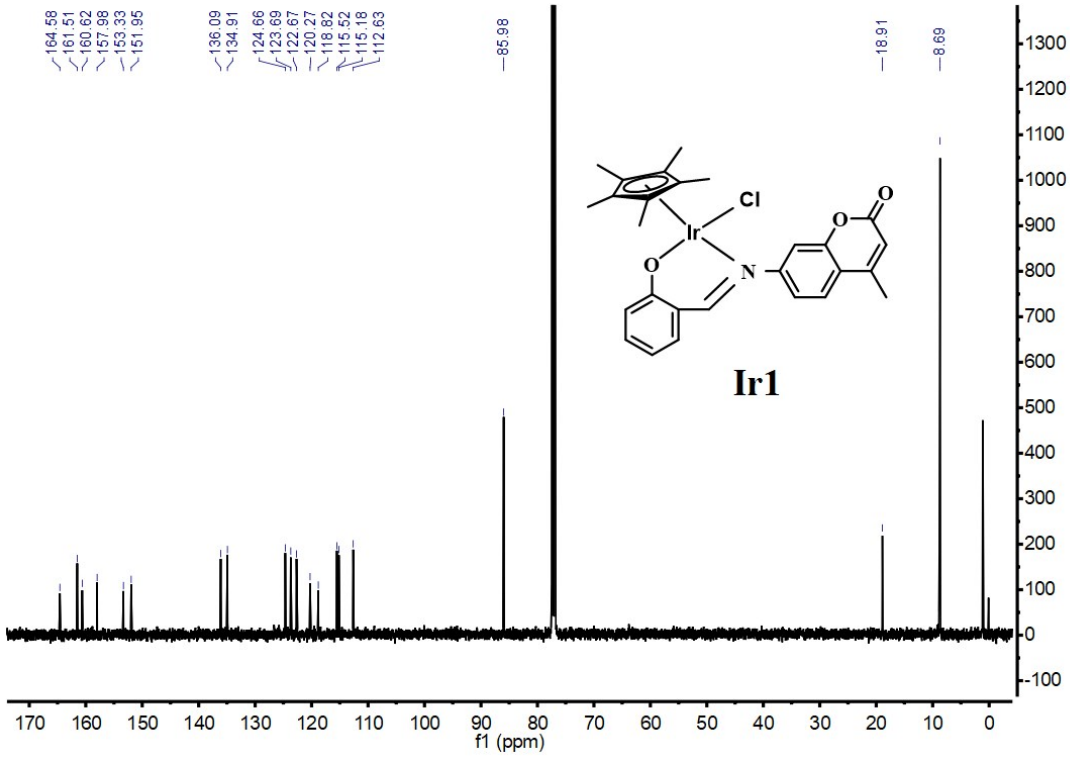
164.58
161.51
160.62
157.98
153.33
151.95
136.09
134.91
124.66
123.69
122.67
120.27
118.82
115.52
115.18
112.63
85.98
18.91
8.69
Cl
Ir
O
N
O
O
Ir1
f1 (ppm)

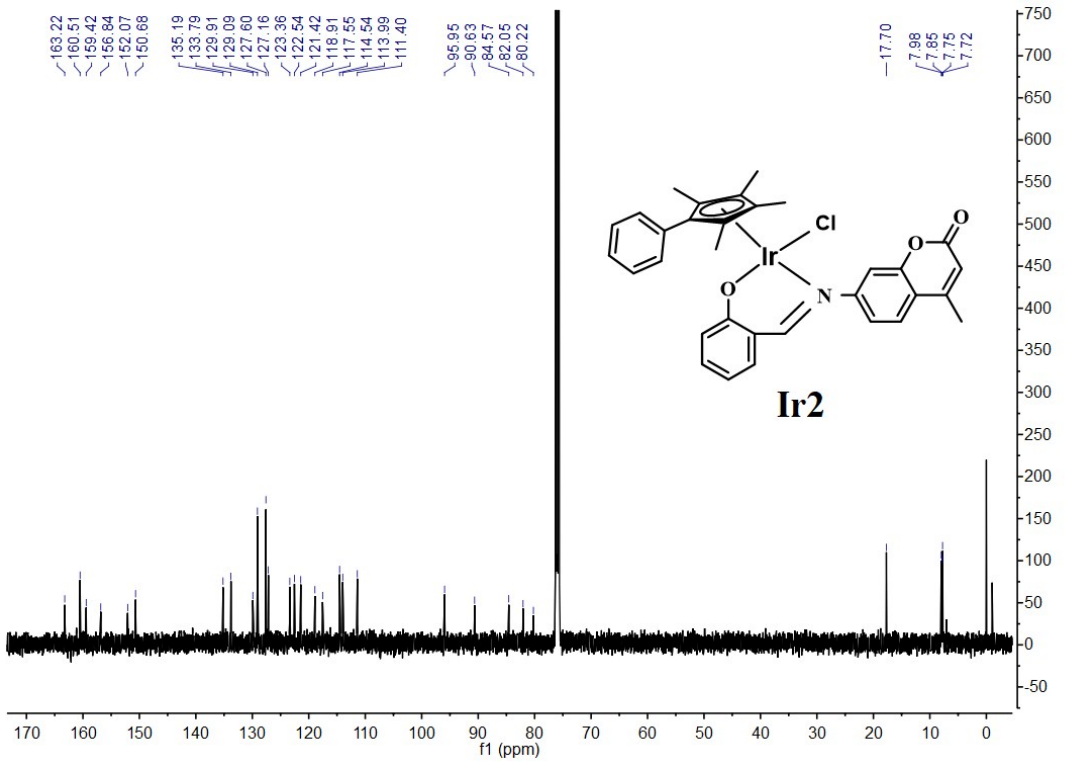
163.22
160.51
159.42
156.84
152.07
150.68
135.19
133.79
129.91
129.09
127.60
127.16
123.36
122.54
121.42
118.91
117.55
114.54
113.99
111.40
95.95
90.63
84.57
82.05
80.22
17.70
7.98
7.85
7.75
7.72
Cl
Ir
O
N
O
O
Ir2
f1 (ppm)

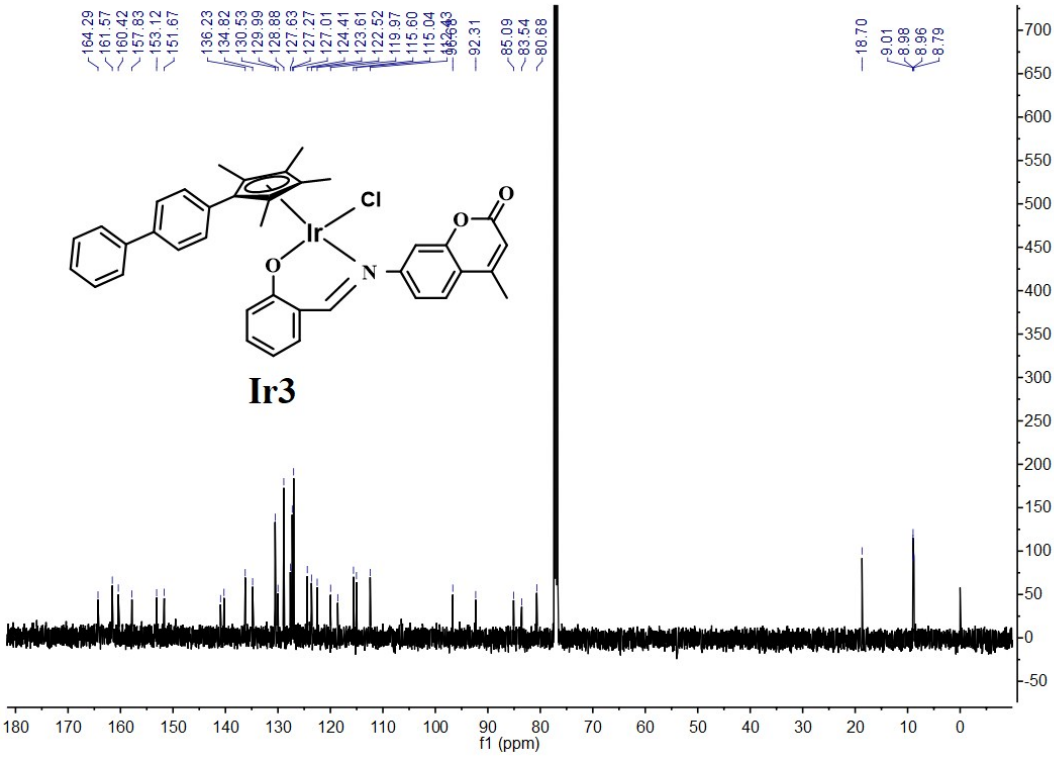
164.29
161.57
160.42
157.83
153.12
151.67
136.23
134.82
130.53
129.99
128.88
127.63
127.27
127.01
124.41
123.61
122.52
119.97
115.60
115.04
92.31
85.09
83.54
80.68
18.70
9.01
8.98
8.96
8.79
Cl
Ir
O
N
O
O
Ir3
f1 (ppm)

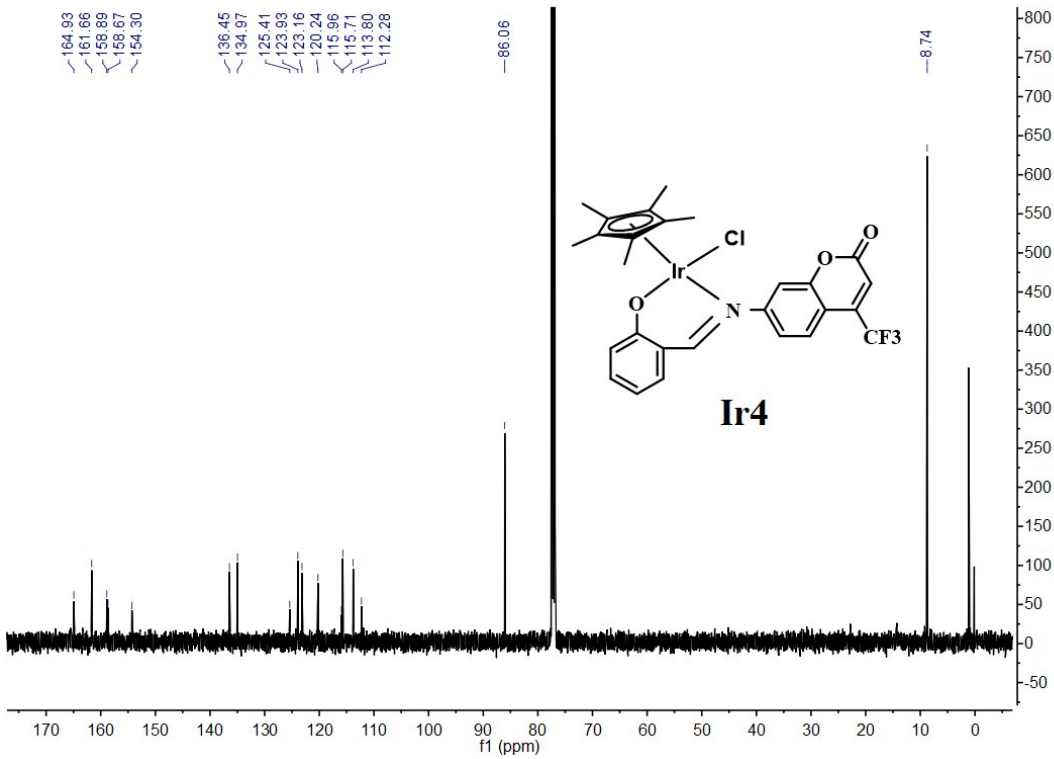
164.93
161.66
158.89
158.67
154.30
136.45
134.97
125.41
123.93
123.16
120.24
115.96
115.71
113.80
112.28
86.06
8.74
Cl
Ir
O
N
O
O
CF3
Ir4
f1 (ppm)

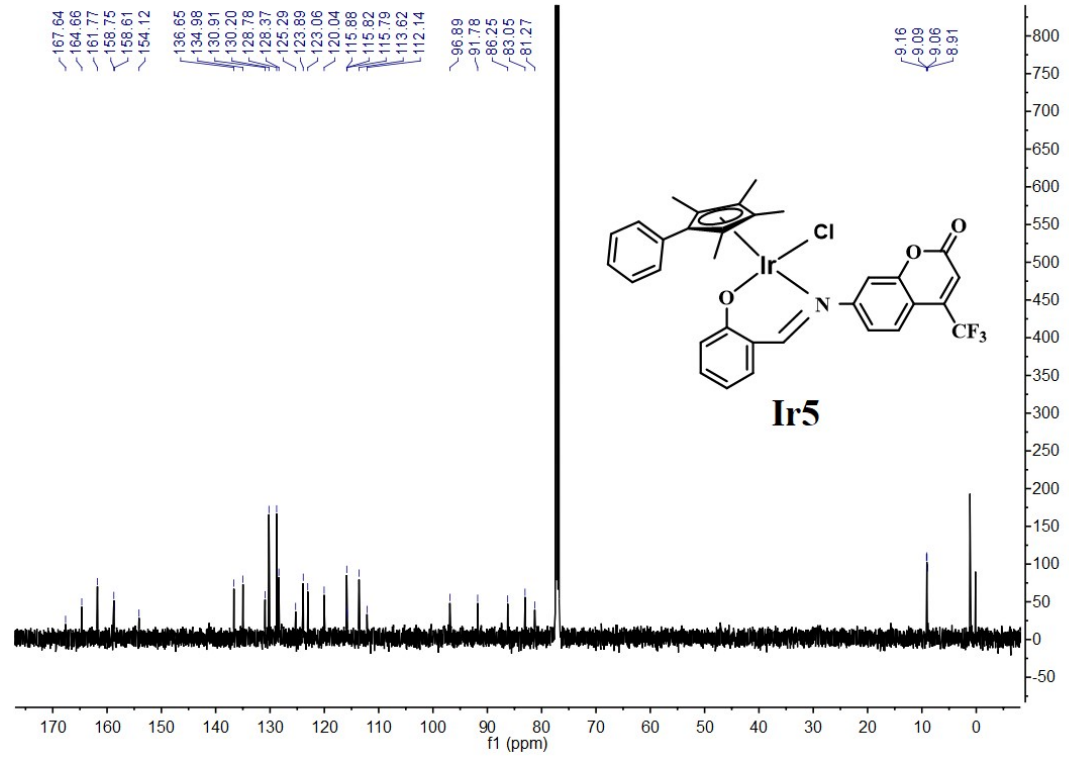


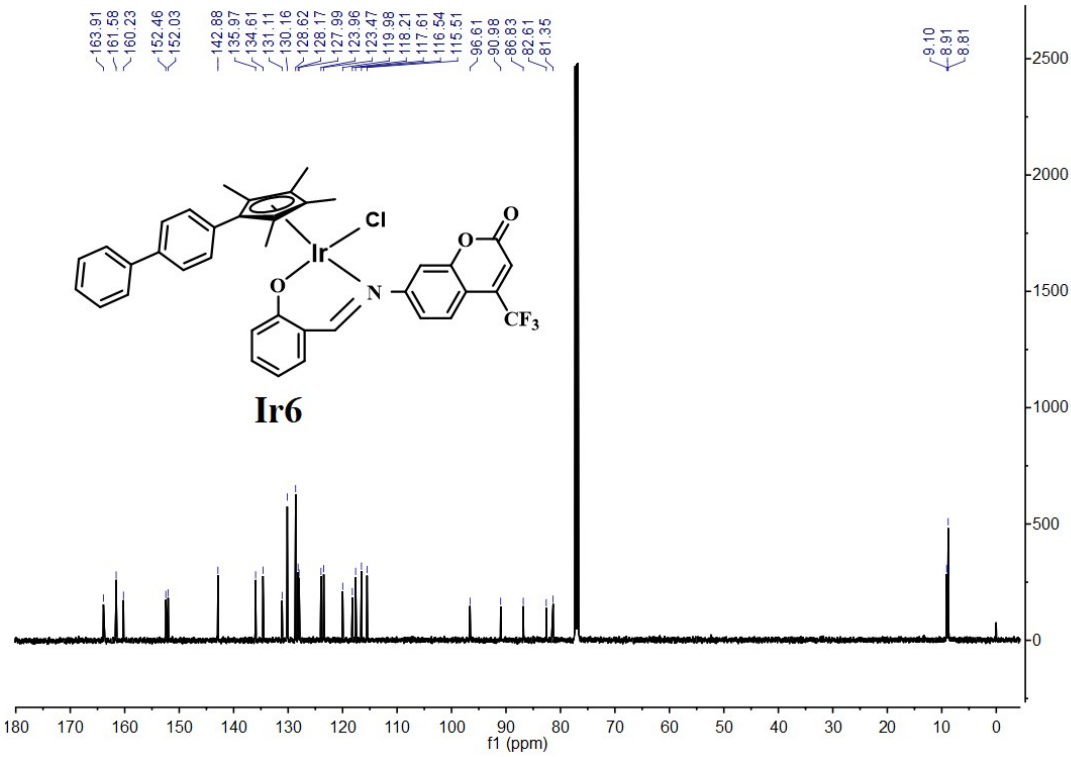


**Figure S3.** $^{13}$C NMR spectra (126 MHz) of **Ir1-Ir6**.

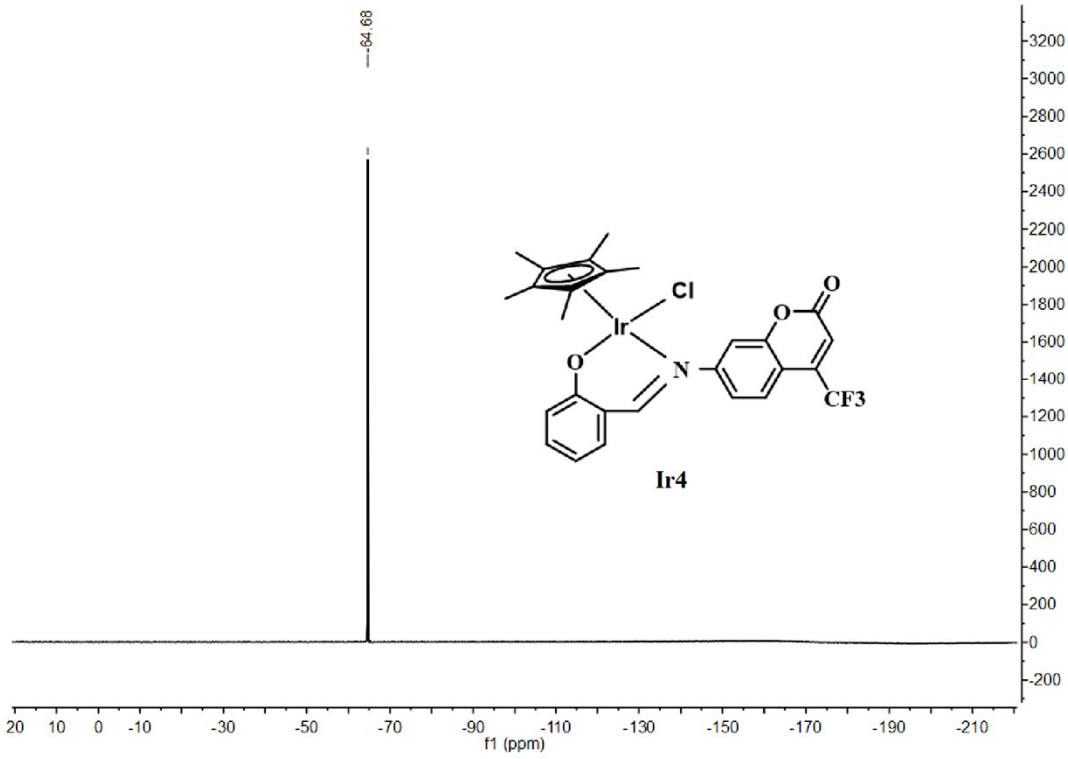
-64.68
Cl
Ir
O
N
O
O
CF3
Ir4
3200
3000
2800
2600
2400
2200
2000
1800
1600
1400
1200
1000
800
600
400
200
0
-200
20 10 0 -10 -30 -50 -70 -90 -110 -130 -150 -170 -190 -210
f1 (ppm)

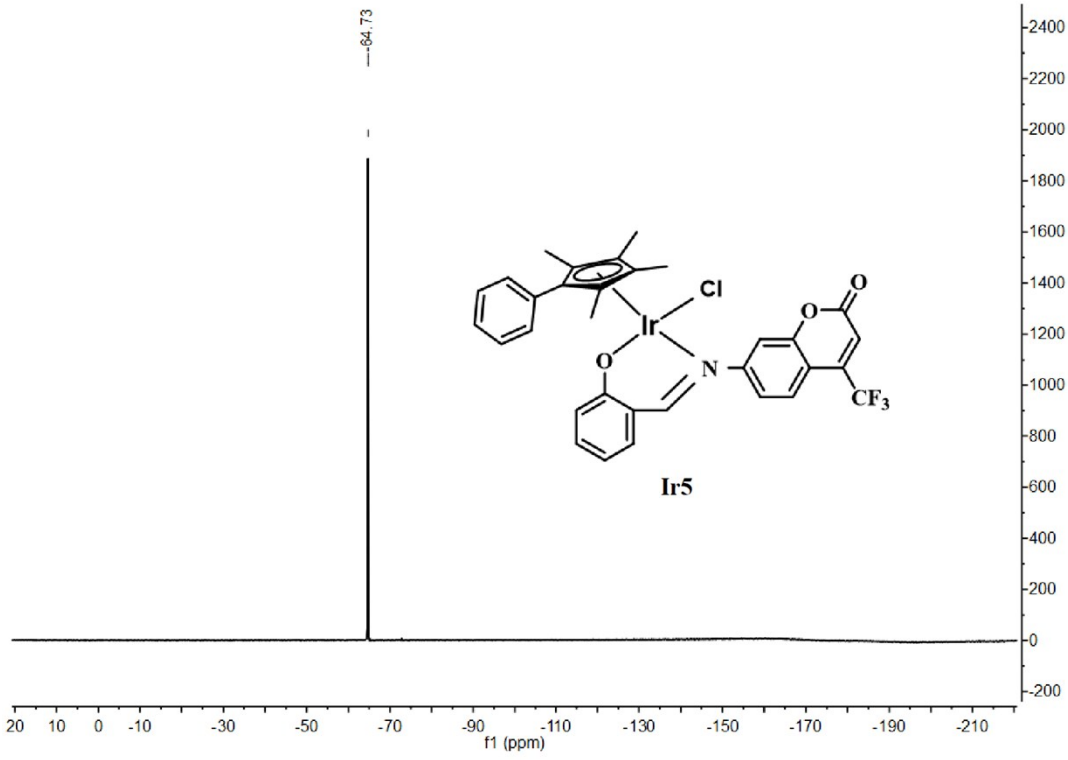
-64.73
Cl
Ir
O
N
O
O
CF3
Ir5
2400
2200
2000
1800
1600
1400
1200
1000
800
600
400
200
0
-200
20 10 0 -10 -30 -50 -70 -90 -110 -130 -150 -170 -190 -210
f1 (ppm)

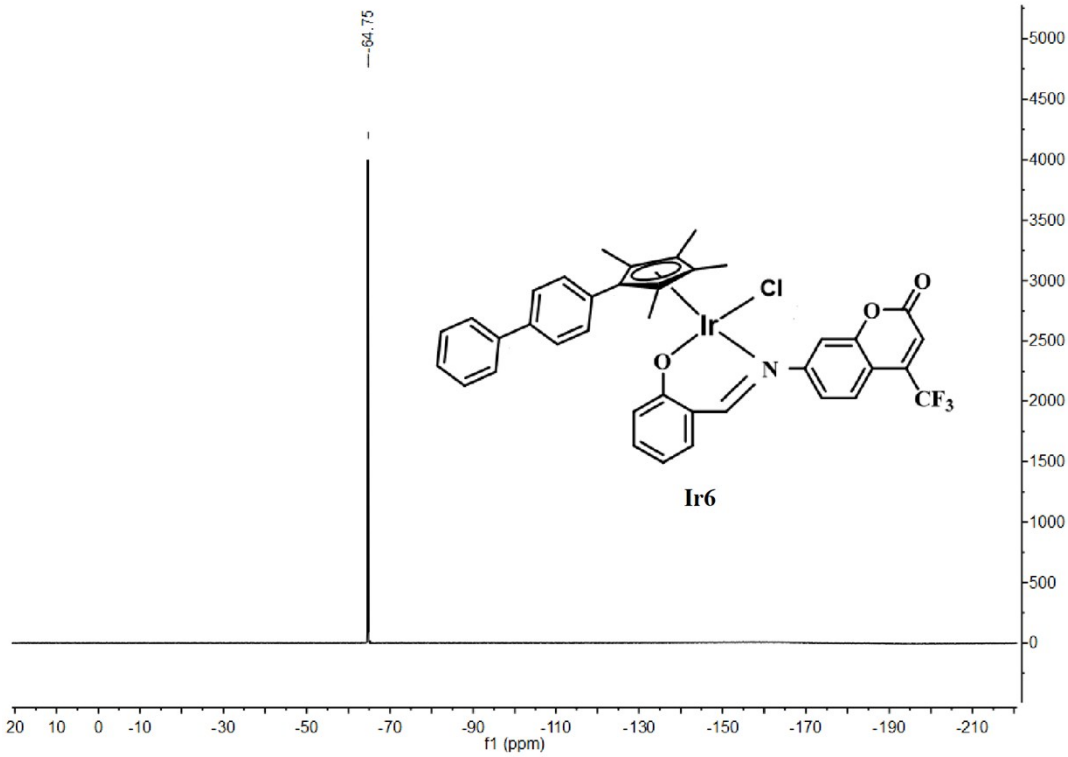


**Figure S4.** $^{19}$F NMR spectra (471 MHz) of **Ir4-Ir6**.

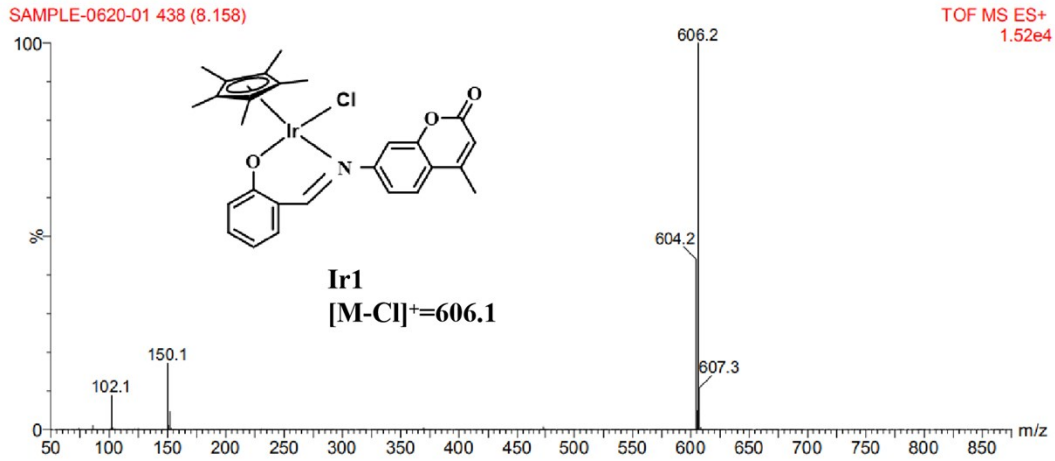

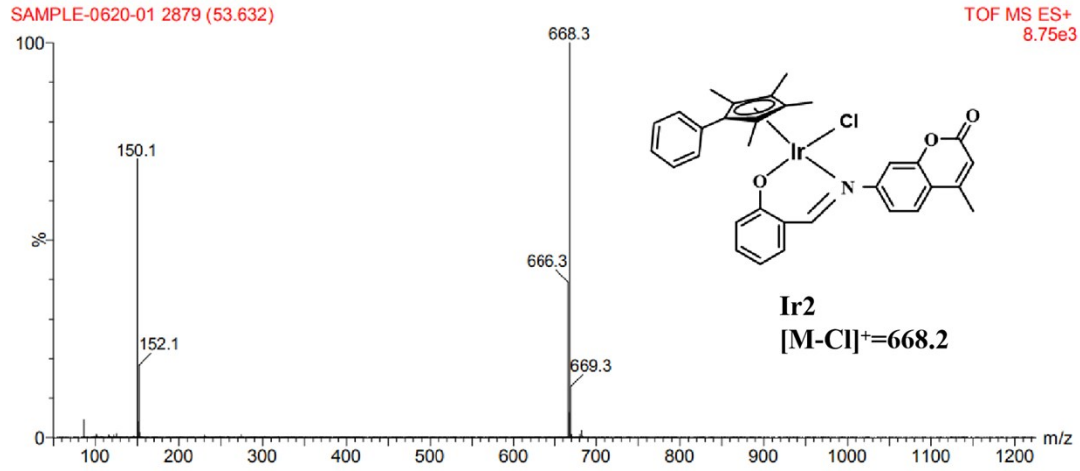
SAMPLE-0620-01 2879 (53.632)
TOF MS ES+
8.75e3
668.3
150.1
666.3
152.1
669.3
Cl
Ir
O
N
O
O
Ir2
[M-Cl]+=668.2
m/z

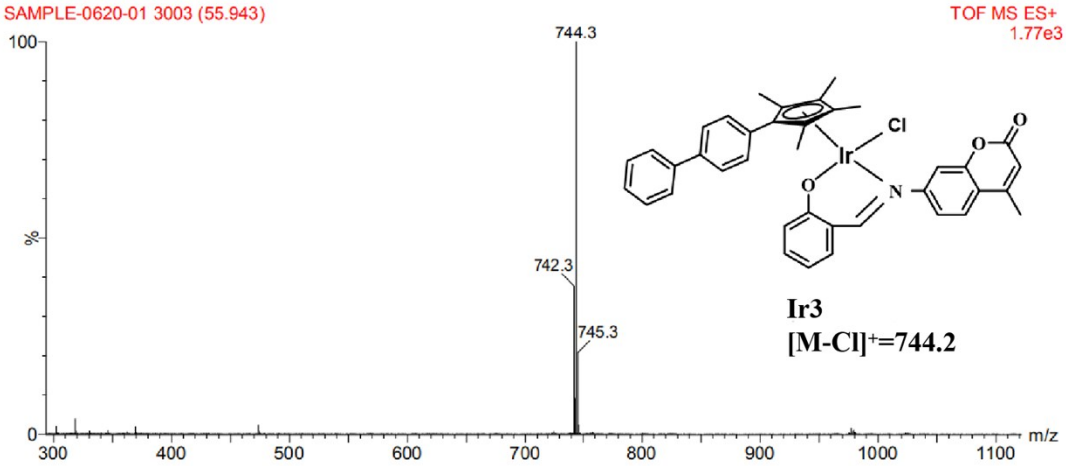
SAMPLE-0620-01 3003 (55.943)
TOF MS ES+
1.77e3
744.3
742.3
745.3
Cl
Ir
O
N
O
O
Ir3
[M-Cl]+=744.2
m/z

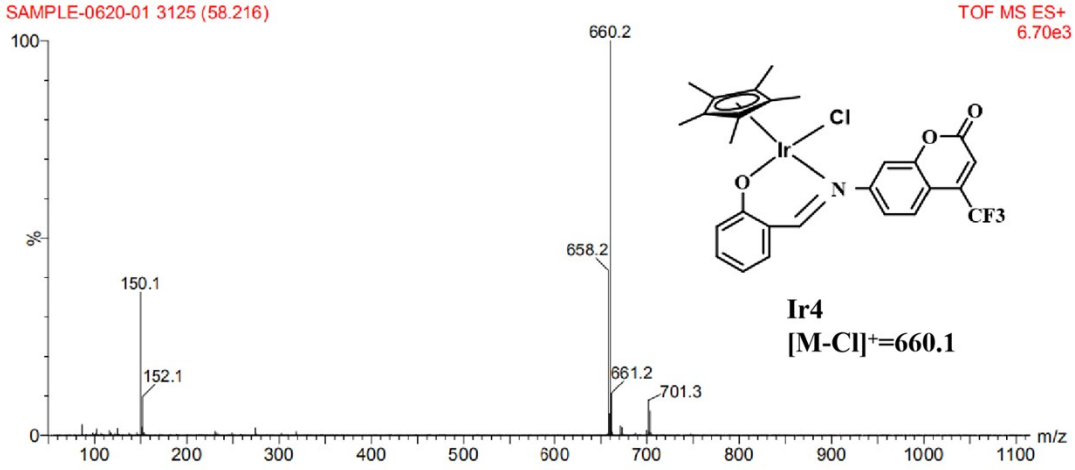
SAMPLE-0620-01 3125 (58.216)
TOF MS ES+
6.70e3
660.2
658.2
150.1
152.1
661.2
701.3
Cl
Ir
O
N
O
O
CF3
Ir4
[M-Cl]+=660.1
m/z

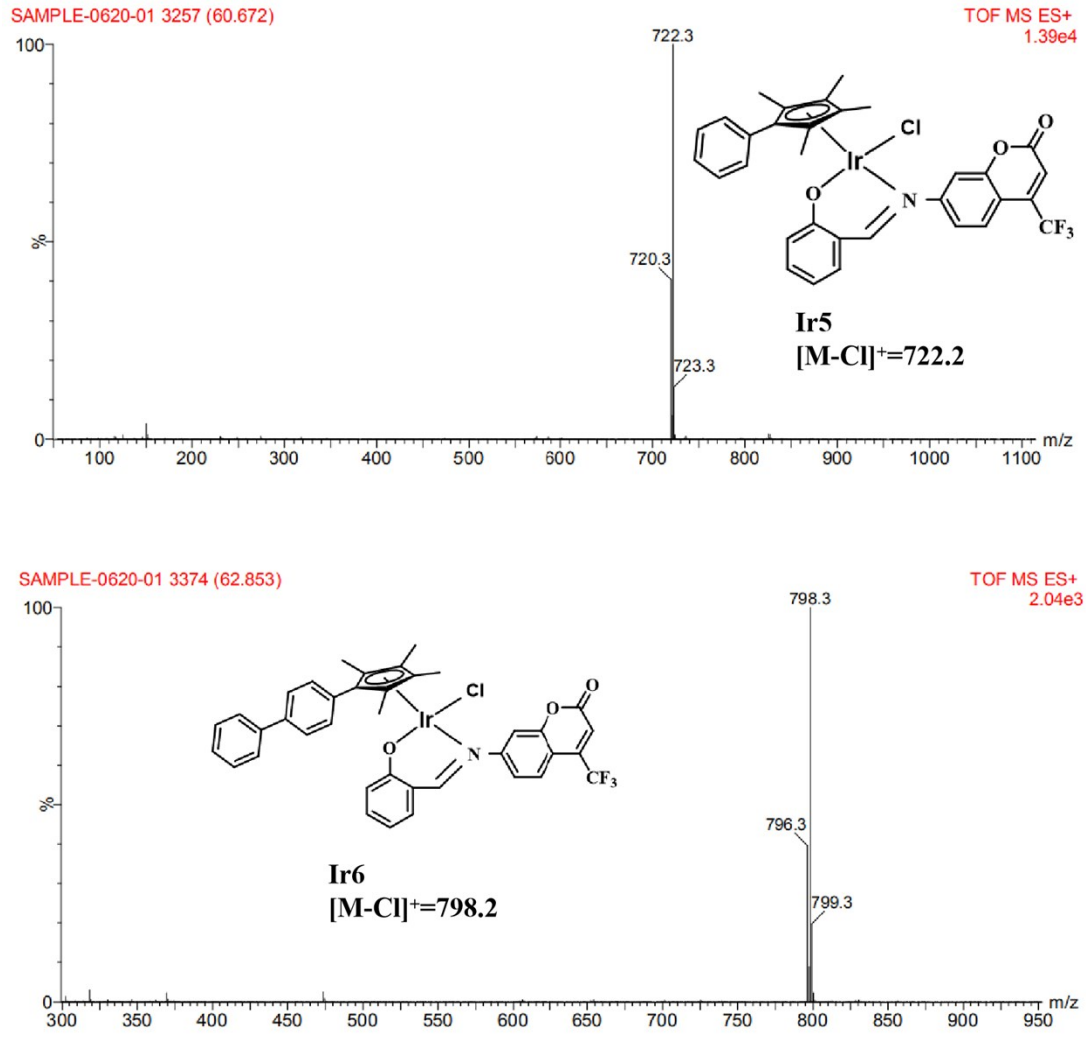


**Figure S5.** ESI-MS spectra of **Ir1-Ir6**.

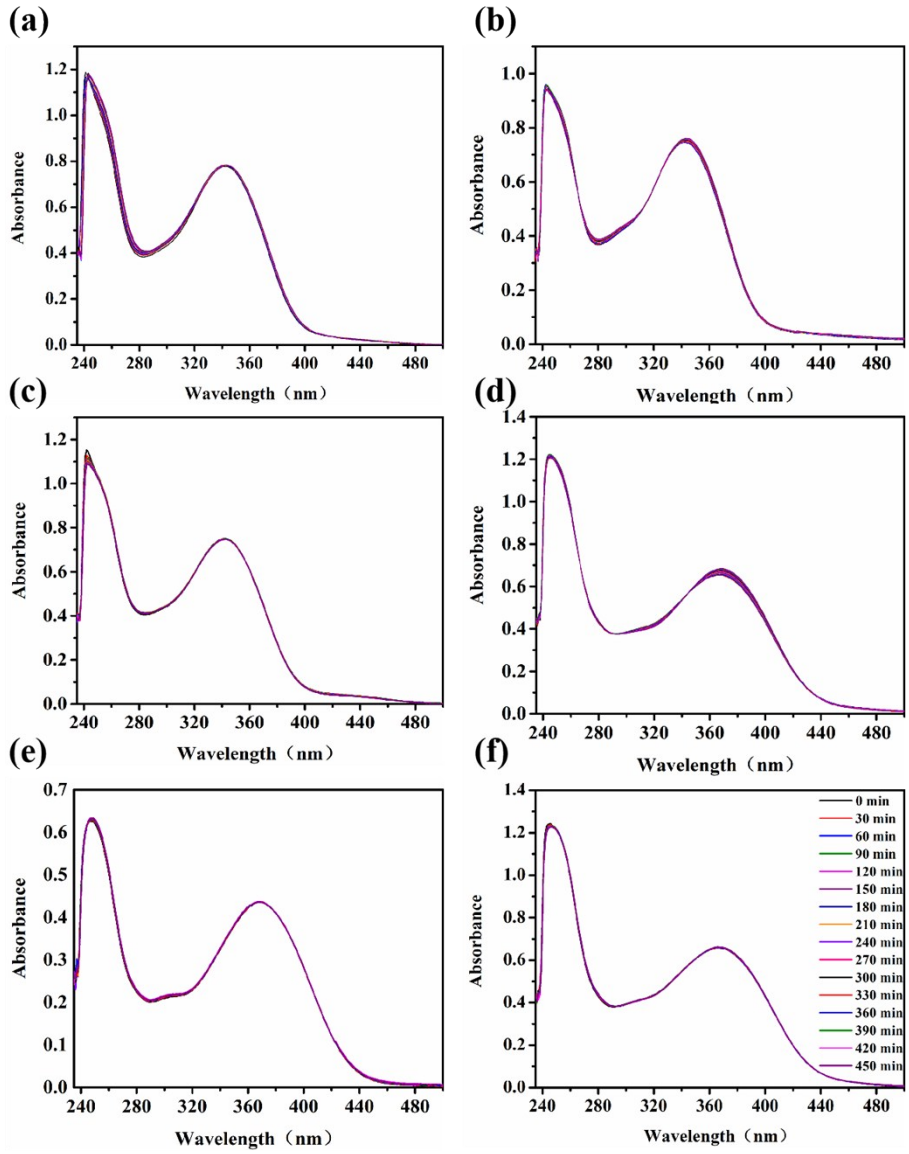


**Figure S6.** UV-vis spectra for of **Ir1** (a), **Ir2** (b), **Ir3** (c), **Ir4** (d), **Ir5** (e), **Ir6** (f) in 20% DMSO/80% $H_2O$ (*v*/*v*) recorded over 8 h at 298 K.

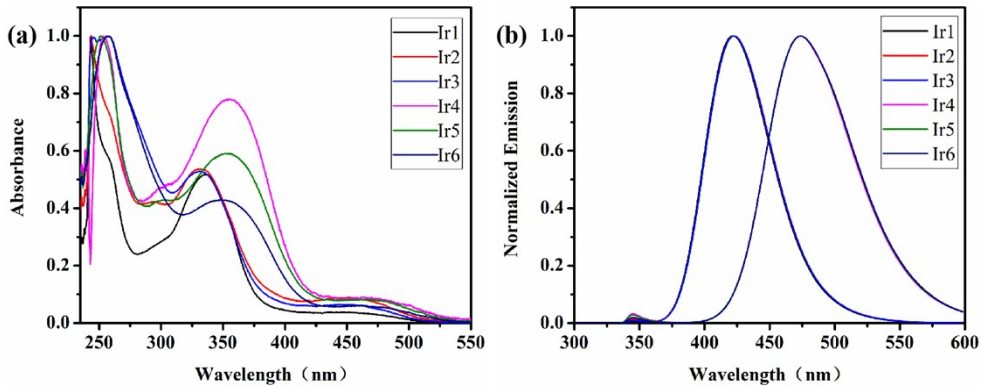

**Figure S7.** UV−vis spectra (a) and fluorescence spectra (b) of **Ir1-Ir6** (20 $\mu$M) in DMSO solution.

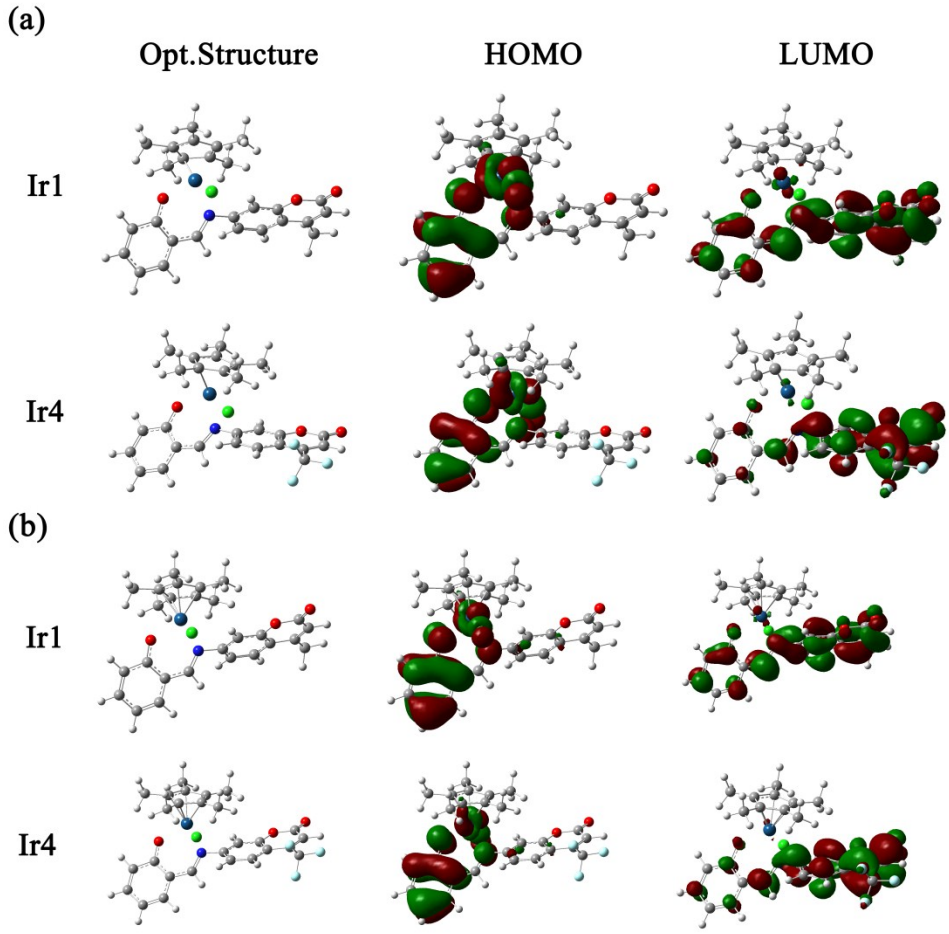


**Figure S8.** Electron cloud distribution (isovalue=0.03) of HOMO and LUMO orbits of **Ir1** and **Ir4** (a) at the level of B3LYP//6-311G(d,p)/LANL2TZf, (b) at the level of M06-2X//6-311G(d,p)/LANL2TZf.

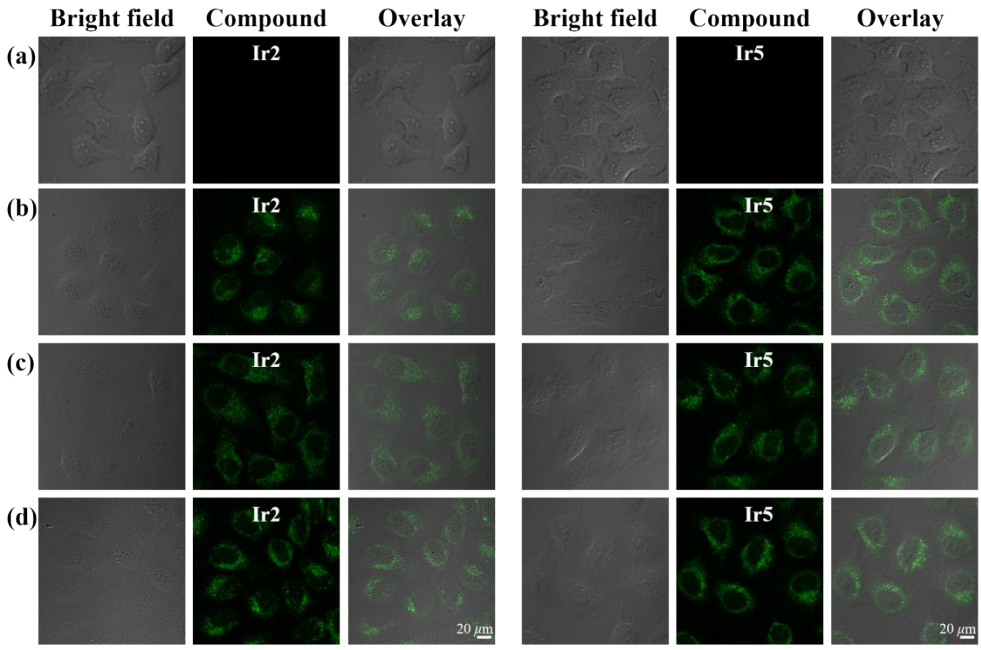


**Figure S9.** Confocal images of A549 cells after hatched in **Ir2** and **Ir5** (10 $\mu$M) under different conditions. The cells were treated with (a) at 277 K for 10 min; (b) at 310 K for 10 min; (c) exposed to CCCP (10 $\mu$M) at 310 K for 1 h; (d) exposed to chloroquine (50 $\mu$M) at 310 K for 1 h. ($\lambda ex$ = 405 nm, $\lambda em$ = 430-490 nm). Scale bars: 20 $\mu$m.

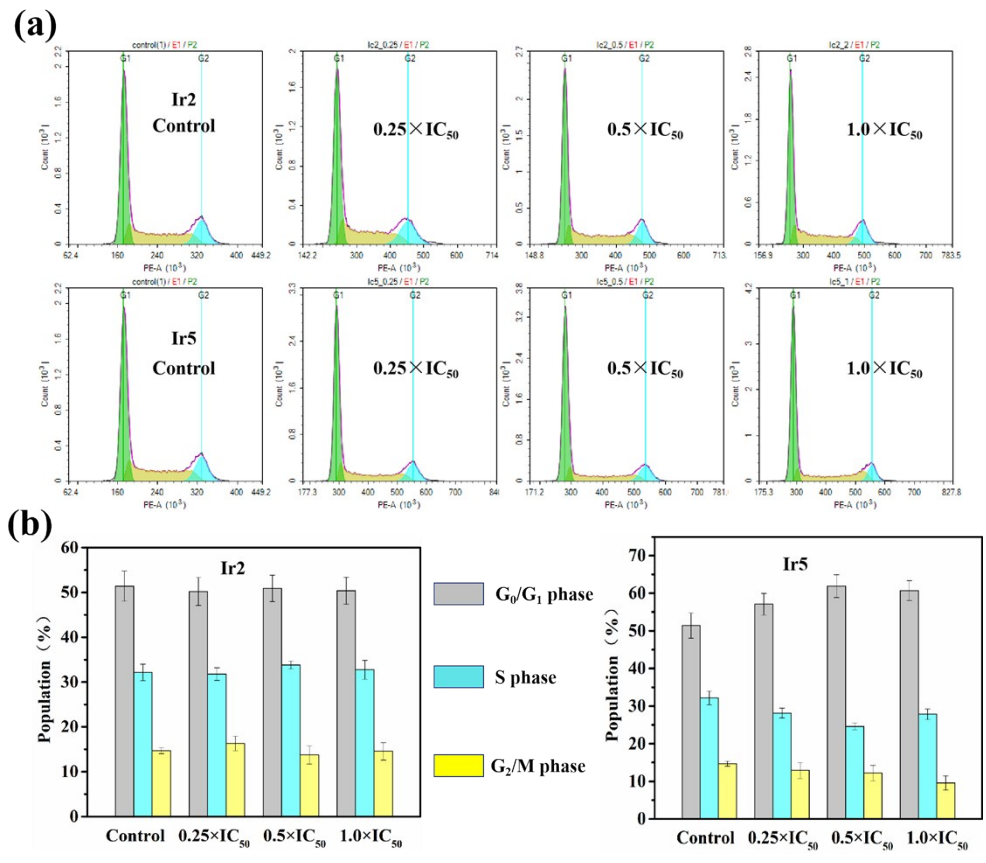

**Figure S10.** (a) Flow cytometry data for cell cycle distribution of A549 cells exposed to **Ir2** and **Ir5** for 24 h. Concentrations used were 0.25 × $IC_{50}$, 0.5 × $IC_{50}$, 1.0 × $IC_{50}$. Cell staining for flow cytometry was carried out using PI/RNase. Cell populations in each cell cycle phase for control. (b) Histogram of Flow cytometry data for cell cycle distribution of A549 cancer cells exposed to **Ir2** and **Ir5** for 24 h. Data are quoted as mean ± SD of three replicates.

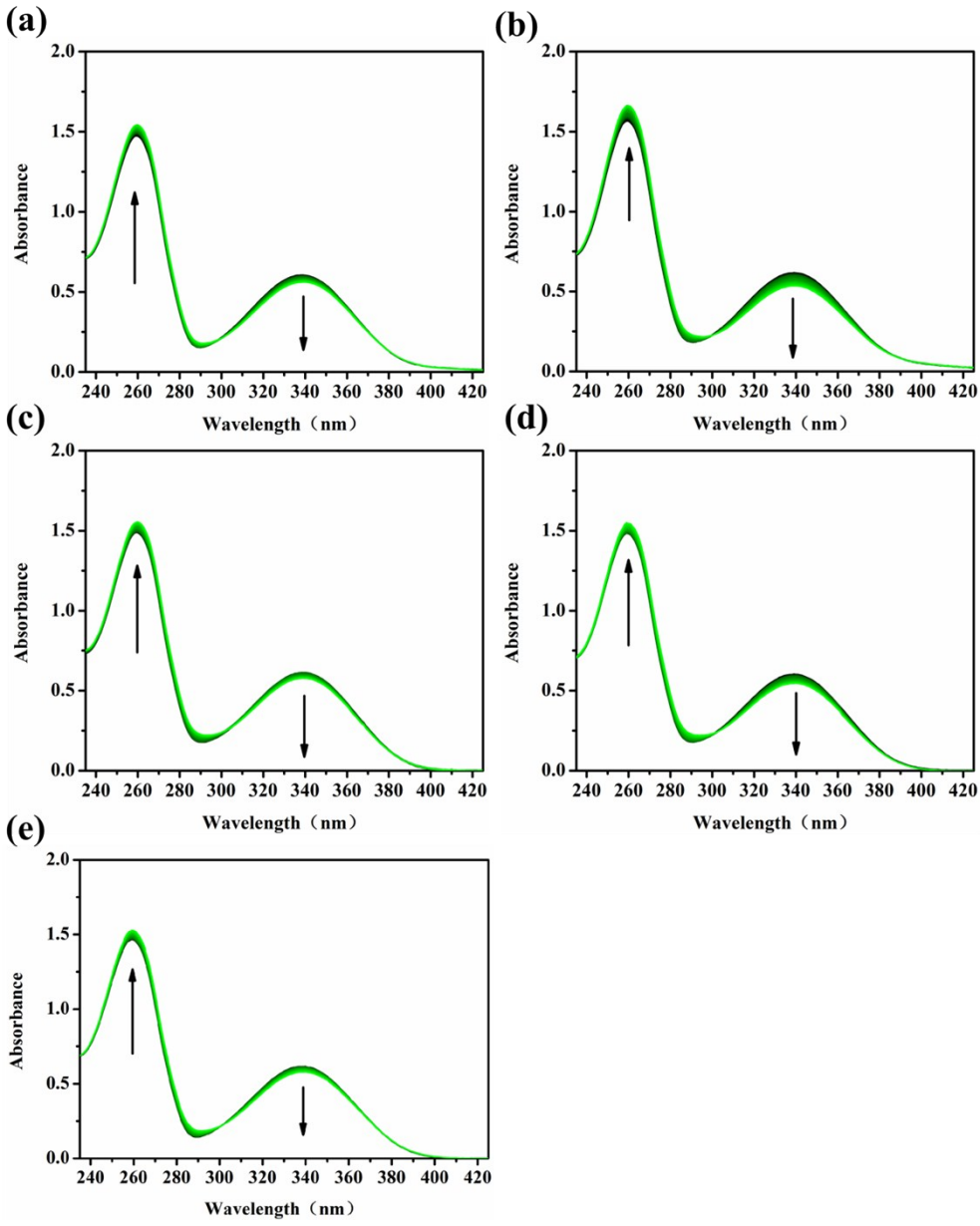


**Figure S11**. UV-vis spectra of of NADH (100.0 $\mu$M) catalyzed by **Ir1** (a), **Ir3** (b), **Ir4** (c), **Ir5** (d), **Ir6** (e) (1.0 $\mu$M) in 10% MeOH/90% $H_2O$ (*v*:*v*) at 298 K over 8 h.

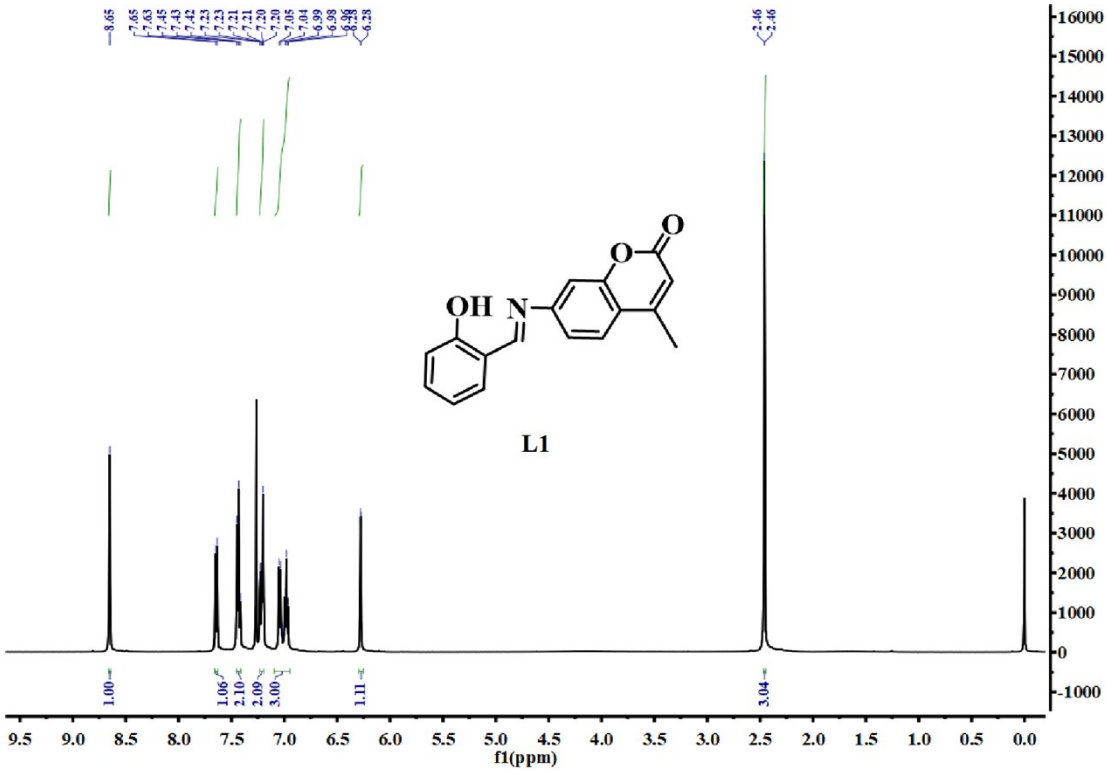
8.65
7.65
7.63
7.45
7.43
7.42
7.23
7.21
7.20
7.05
7.04
6.99
6.98
6.38
6.23
2.46
2.46
OH
N
O
O
L1
1.00
1.06
2.10
2.09
3.00
1.11
3.04
f1(ppm)

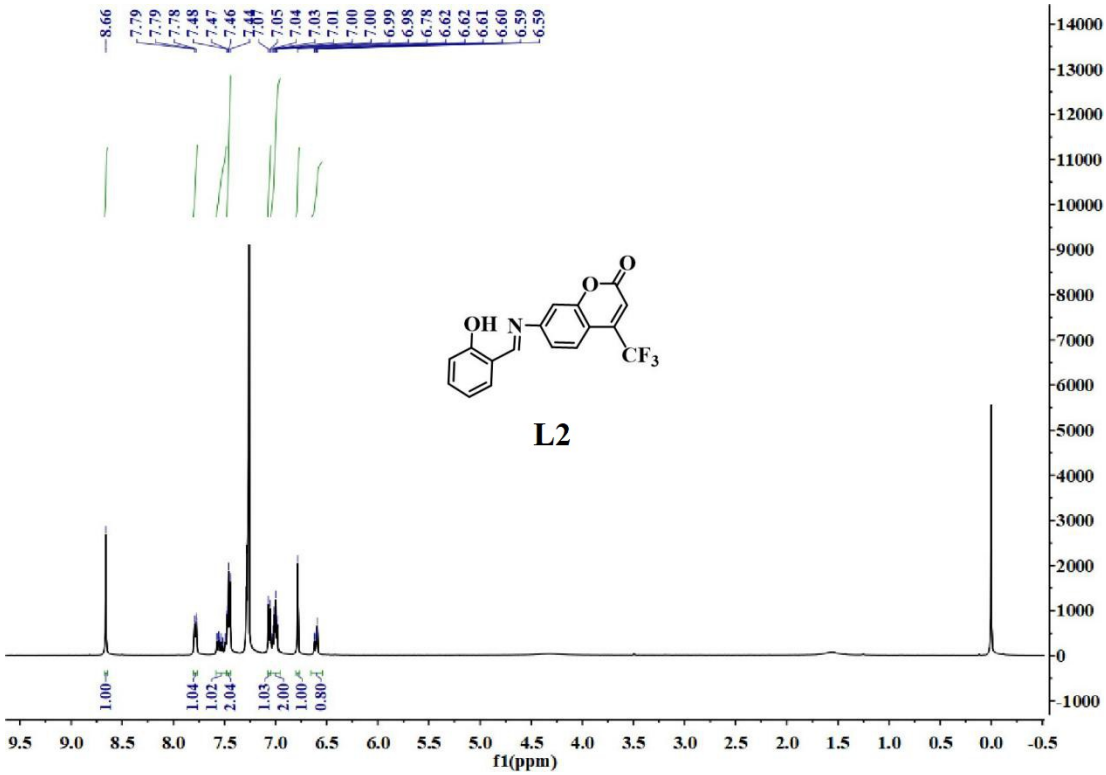


**Figure S12.** $^{1}$H NMR (500 MHz) of **L1** and **L2**.

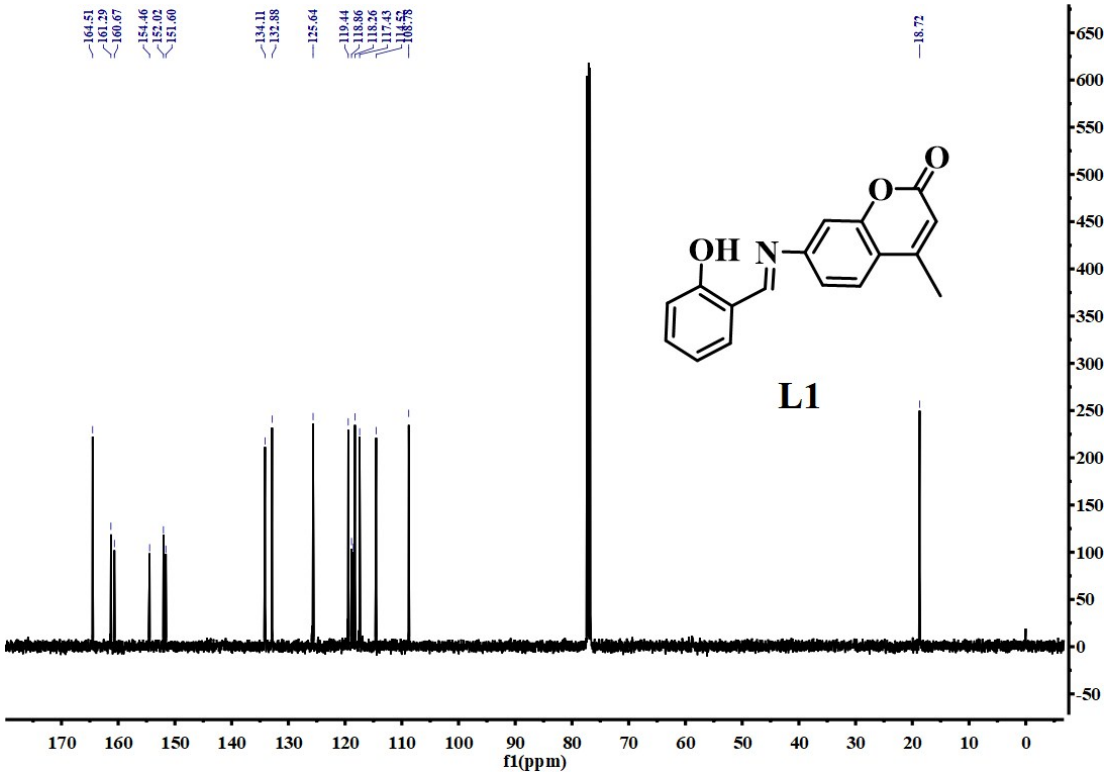

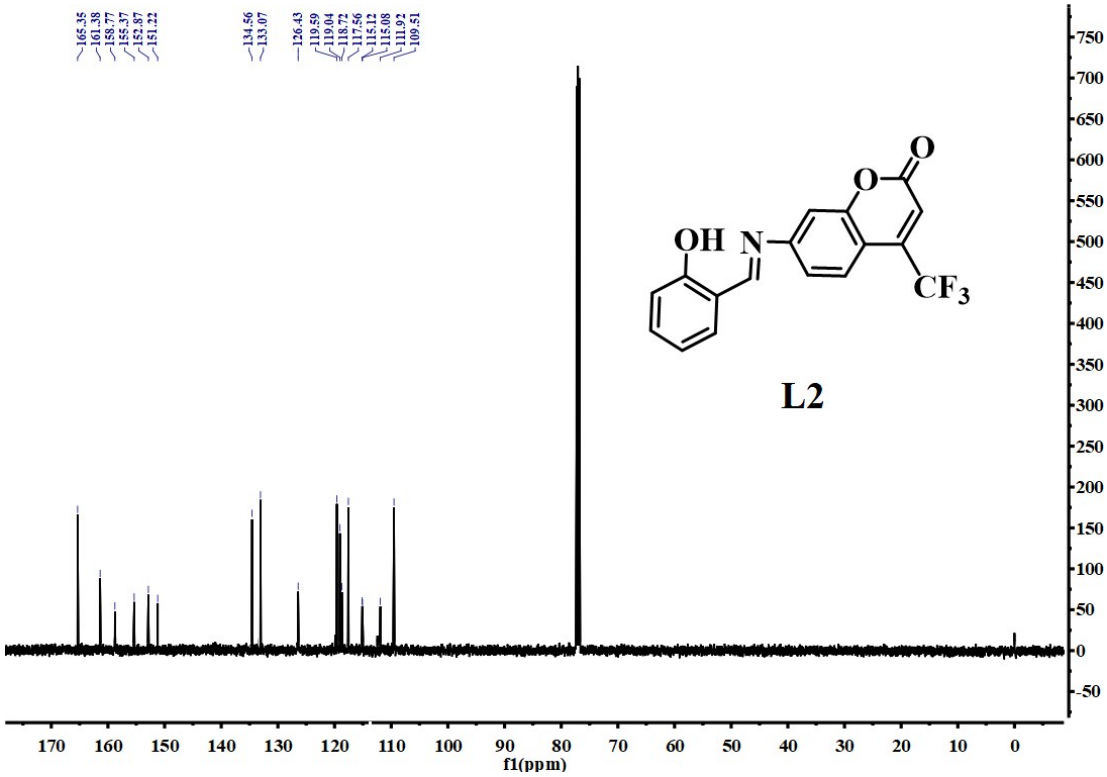


**Figure S13.** $^{13}C$ NMR (126 MHz) of **L1** and **L2**.

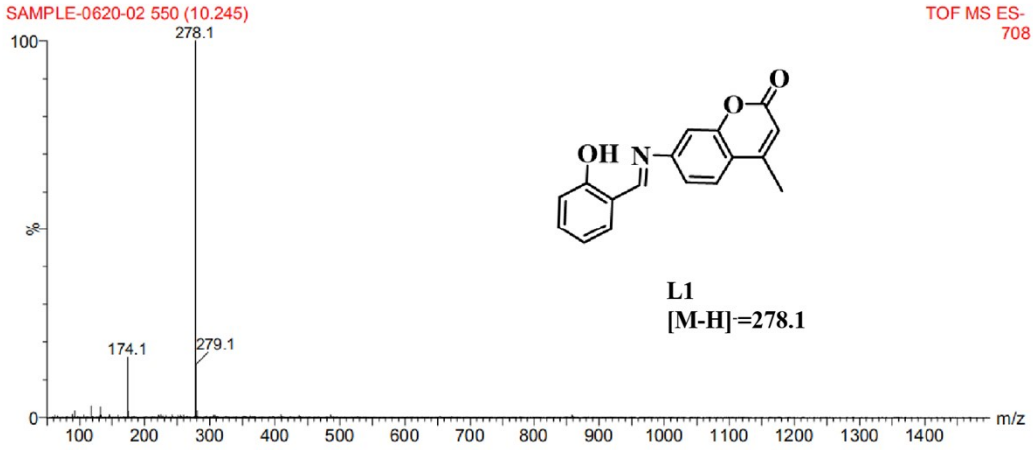

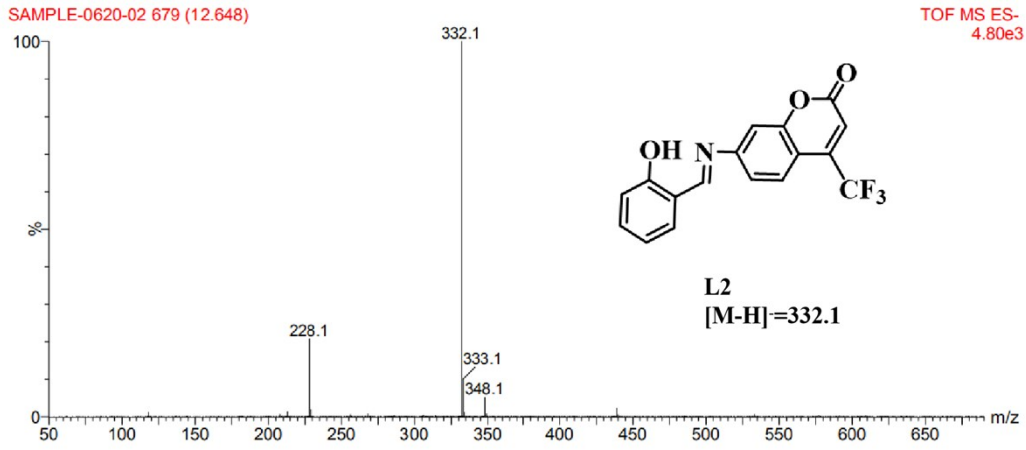


**Figure S14.** ESI-MS spectra of **L1, L2**.

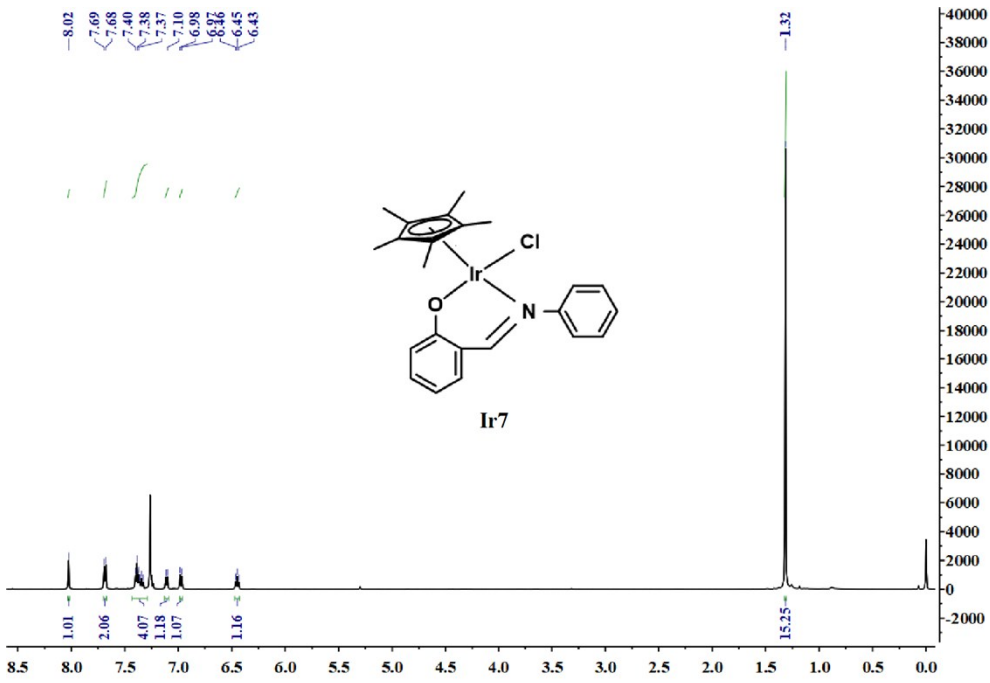


**Figure S15.** $^{1}$H NMR (500 MHz) of **Ir7**.

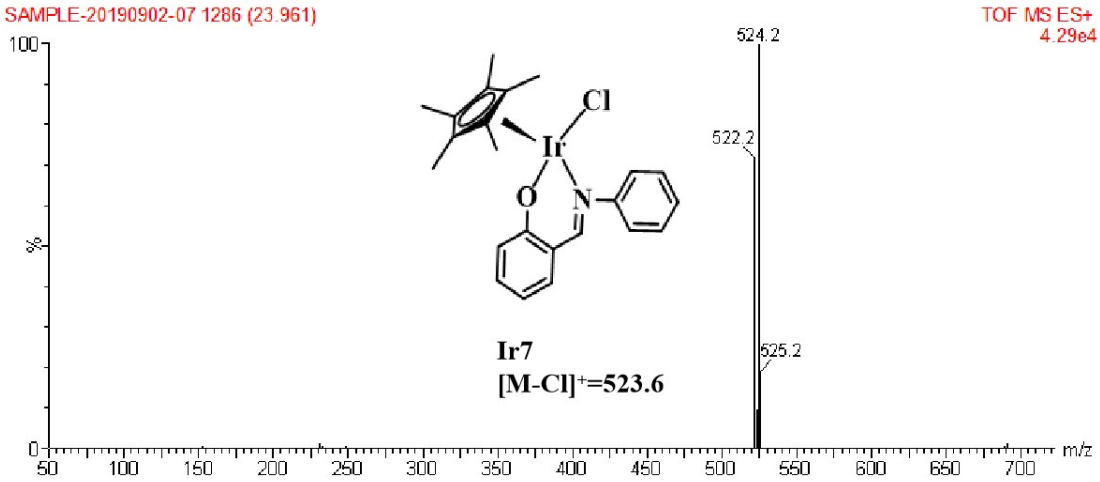


**Figure S16.** ESI-MS spectra of **Ir7**.

**Table S1**. Crystallographic data for **Ir1** and **Ir4**.

| Compound | Ir1 | Ir4 |
|---|---|---|
| Formula | $C_{27}H_{27}ClIrNO_3$ | $C_{27}H_{24}ClF_3IrNO_3$ |
| MW | 641.15 | 695.12 |
| Crystal size (mm) | 0.35×0.20×0.10 | 0.32×0.17×0.01 |
| $\lambda$(Å) | 0.71073 | 0.71073 |
| Temperature (K) | 298 | 298 |
| Crystal system | Triclinic | Monoclinic |
| Space group | P-1 | P2(1)/c |
| a (Å) | 8.2136(8) | 13.4707(11) |
| b (Å) | 9.9605(9) | 19.1603(16) |
| c (Å) | 15.7811(12) | 10.0964(9) |
| $\alpha$ (°) | 76.150(2) | 90 |
| $\beta$ (°) | 79.874(3) | 104.571(2) |
| $\gamma$ (°) | 71.8540(10) | 90 |

| | | |
|---|---|---|
| Volume ($Å^3$ ) | 1184.00(18) | 2522.1(4) |
| *Z* | 2 | 4 |
| density (calc) ($Mg \cdot m^{-3}$) | 1.798 | 1.831 |
| abs coeff ($mm^{-1}$) | 5.781 | 5.452 |
| F(000) | 628 | 1352 |
| $\theta$ range (deg) | 2.33 to 25.02 | 2.34 to 25.02 |
| index ranges | -9≤h≤9, -11≤k≤11, -15≤l≤18 | -16≤h≤15, -19≤k≤22, -10≤l≤12 |
| reflns collected | 5871 | 12449 |
| indep reflns | 4085 [R(int) = 0.0365] | 4425 [R(int) = 0.0349] |
| data / restraints / params | 4085 / 0 / 304 | 4425 / 0 / 330 |
| final R indices [I > 2σ(I)] | R1 = 0.0492, wR2 = 0.1306 | R1 = 0.0253, wR2 = 0.0564 |
| GOF | 1.052 | 1.058 |
| largest diff peak and hole | 2.107 and -3.289 | 0.543 and -1.184 |

**Table S2**. Selected distances (Å) and angles (°) between atoms for **Ir1** and **Ir4**.

| **bond/angle** | **Ir1** | **Ir4** |
|---|---|---|
| Ir–C (Cp*ring) | 2.102(9) | 2.127(4) |
| | 2.148(9) | 2.138(4) |
| | 2.161(10) | 2.162(5) |
| | 2.169(10) | 2.168(4) |
| | 2.182(8) | 2.169(4) |
| Ir–CP(centroid) | 1.7741 | 1.7717 |
| $Ir\text{-}N_1$ | 2.100(8) | 2.107(3) |
| $Ir\text{-}O_1$ | 2.072(6) | 2.081(3) |
| $Ir\text{-}Cl_1$ | 2.416(2) | 2.4099(11) |

| | | |
|---|---|---|
| $O_1$-Ir-$N_1$ | 87.9(3) | 85.74(12) |
| $O_1$-Ir-$Cl_1$ | 83.8(2) | 84.58(10) |
| $N_1$-Ir-$Cl_1$ | 86.7(2) | 90.25(9) |

**Table S3**. UV–vis absorption peaks along with the oscillator strength (f) and orbitals involved in the electronic transition of **Ir1** and **Ir4**, obtained by TDDFT methods (M06-2X/6-311G(d,p)/LANL2TZf //M06-2X/6-311G(d,p)/LANL2TZf)

| Compounds | | Major assignments | Oscillation strength | Calc. (nm) | Expt. (nm) |
|---|---|---|---|---|---|
| Ir1 | S1 | HOMO→LUMO+2 (25%) | 0.0779 | 372 | 336 |
| Ir4 | S1 | HOMO→LUMO (55%) | 0.2394 | 376 | 356 |

**Table S4**. Flow cytometry analysis to determine the percentages of apoptotic A549 cells, using Annexin V-FITC/PI staining after exposure to **Ir2**.

| | Ir concentration | Population (%) | | | |
|---|---|---|---|---|---|
| | | Viable | Early apoptosis | Late apoptosis | Non-viable |
| **control** | | 95.29±1.44 | 0.36±0.30 | 3.32±0.29 | 1.03±0.33 |
| | 1.0 × $IC_{50}$ | 87.42±1.05 | 0.26±0.59 | 8.37±2.53 | 3.95±1.66 |
| **Ir2** | 2.0 × $IC_{50}$ | 82.95±2.51 | 0.61±0.99 | 15.94±2.12 | 0.51±1.01 |

| | | | | | |
|---|---|---|---|---|---|
| | 3.0 × $IC_{50}$ | 63.23±1.21 | 2.40±2.95 | 26.46±1.35 | 7.91±3.19 |

**Table S5**. Flow cytometry analysis to determine the percentages of apoptotic A549 cells, using Annexin V-FITC/PI staining after exposure to **Ir5**.

| | **Ir concentration** | **Population (%)** | | | |
|---|---|---|---|---|---|
| | | **Viable** | **Early apoptosis** | **Late apoptosis** | **Non-viable** |
| **control** | | 95.29±1.44 | 0.36±0.30 | 3.32±0.29 | 1.03±0.33 |
| | 1.0 × $IC_{50}$ | 88.29±2.10 | 0.49±0.89 | 8.31±1.59 | 2.90±1.69 |
| **Ir5** | 2.0 × $IC_{50}$ | 72.87±1.36 | 1.14±1.56 | 13.84±2.69 | 12.15±0.96 |
| | 3.0 × $IC_{50}$ | 48.69±1.78 | 0.84±1.98 | 32.52±2.11 | 17.94±2.26 |

**Table S6**. A549 cell cycle analysis carried out by flow cytometry using PI staining after exposure to **Ir2**.

| | **Ir concentration** | **Population (%)** | | |
|---|---|---|---|---|
| | | **$G_0/G_1$ phase** | **S phase** | **$G_2$/M phase** |
| **control** | | 51.41±3.36 | 32.16±1.85 | 14.69±0.65 |
| | 0.25 × $IC_{50}$ | 50.23±3.12 | 31.79±1.42 | 16.33±1.63 |
| **Ir2** | 0.5 × $IC_{50}$ | 50.92±2.96 | 33.83±0.89 | 13.75±2.02 |

| | | | | |
|---|---|---|---|---|
| | $1.0 \times IC_{50}$ | 50.39±3.01 | 32.76±2.11 | 14.56±1.95 |

**Table S7**. A549 cell cycle analysis carried out by flow cytometry using PI staining after exposure to **Ir5**.

| | **Ir concentration** | **Population (%)** | | |
|---|---|---|---|---|
| | | **$G_0/G_1$ phase** | **S phase** | **$G_2$/M phase** |
| **control** | | 51.41±3.36 | 32.16±1.85 | 14.69±0.65 |
| | $0.25 \times IC_{50}$ | 57.09±2.89 | 28.12±1.29 | 12.88±2.12 |
| **Ir5** | $0.5 \times IC_{50}$ | 61.87±3.01 | 24.57±0.95 | 12.2±2.04 |
| | $1.0 \times IC_{50}$ | 60.71±2.65 | 27.85±1.42 | 9.56±1.87 |

**Table S8**. Mitochondrial membrane polarization of A549 cells induced by **Ir2**.

| | **Ir concentration** | **Population (%)** | |
|---|---|---|---|
| | | **JC-1 Aggregates** | **JC-1 Monomers** |
| | $0.25 \times IC_{50}$ | 91.80 | 8.19 |
| **Ir2** | $0.5 \times IC_{50}$ | 88.01 | 11.96 |

| | | | |
|---|---|---|---|
| | 1.0× $IC_{50}$ | 75.59 | 24.35 |
| | 2.0× $IC_{50}$ | 63.23 | 36.66 |
| **Negative Control** | | 94.14 | 5.83 |
| **Positive Control** | | 15.65 | 84.35 |

**Table S9**. Mitochondrial membrane polarization of A549 cells induced by **Ir5**.

| | **Ir concentration** | **Population (%)** | |
|---|---|---|---|
| | | **JC-1 Aggregates** | **JC-1 Monomers** |
| | 0.25 × $IC_{50}$ | 91.30 | 8.69 |
| **Ir5** | 0.5 × $IC_{50}$ | 79.29 | 20.68 |
| | 1.0× $IC_{50}$ | 59.74 | 40.25 |
| | 2.0× $IC_{50}$ | 55.24 | 43.93 |
| **Negative Control** | | 94.14 | 5.83 |
| **Positive Control** | | 15.65 | 84.35 |

Reference：

[1] Gaussian 09, Revision D.01, M. J. Frisch, G. W. Trucks, H. B. Schlegel, G. E.Scuseria, M. A. Robb, J. R. Cheeseman, G. Scalmani, V. Barone, B. Mennucci,G. A. Petersson, H. Nakatsuji, M. Caricato, X. Li, H. P. Hratchian,A. F. Izmaylov, J. Bloino, G. Zheng, J. L. Sonnenberg, M. Hada, M. Ehara,K. Toyota, R. Fukuda, J. Hasegawa, M. Ishida, T. Nakajima, Y. Honda, O.Kitao, H. Nakai, T. Vreven, J. A. Montgomery, Jr. , J. E. Peralta, F. Ogliaro,M. Bearpark, J. J. Heyd, E. Brothers, K. N. Kudin, V. N. Staroverov, T. Keith,R. Kobayashi, J. Normand, K. Raghavachari, A. Rendell, J. C. Burant, S. S.Iyengar, J. Tomasi, M. Cossi, N. Rega, J. M. Millam, M. Klene, J. E. Knox,J. B. Cross, V. Bakken, C. Adamo, J. Jaramillo, R. Gomperts, R. E. Stratmann,O. Yazyev, A. J. Austin, R. Cammi, C. Pomelli, J. W. Ochterski, R. L.Martin, K. Morokuma, V. G. Zakrzewski, G. A. Voth, P. Salvador, J. J. Dannenberg,S. Dapprich, A. D. Daniels, O. Farkas, J. B. Foresman, J. V. Ortiz,J. Cioslowski, and D. J. Fox, Gaussian, Inc., Wallingford CT, 2013.

[2] M. Cossi, V. Barone, B. Mennucci, J. Tomasi, Chem. Phys. Lett. 286 (1998) 253.

[3] B. Mennucci, J. Tomasi, J. Chem. Phys. 106 (1997) 5151.

[4] A.D. Becke, J. Chem. Phys. 98 (1993) 5648.

[5] C.T. Lee, W.T. Yang, R.G. Parr, Phys. Rev. B 37 (1988) 785.

[6] J.Autschbach, T. Ziegler, S.J.A. Gisbergen, E.J. Baerends,J. Chem. Phys. 116 (2002) 6930.

[7] T. Helgaker, P. Jørgemsen, J. Chem. Phys. 95 (1991) 2595.

[8] Y. Zhao, D.G. Truhlar, Theor. Chem. Acc. 120 (2008) 215.